

# Electrochemically formed fullerene-based polymeric films

Krzysztof Winkler · Alan L. Balch ·  
Włodzimierz Kutner

Received: 11 April 2006 / Revised: 8 May 2006 / Accepted: 8 May 2006 / Published online: 21 July 2006  
© Springer-Verlag 2006

**Abstract** The recent results of investigations involving the electrochemical formation of polymers containing fullerenes and studies of their properties and applications are critically reviewed. From a structural point of view, these polymers can be divided into four main categories including (1) polymers with fullerenes physically incorporated into the foreign polymeric network without forming covalent bonds, (2) fullerene homopolymers formed via [2+2] cycloaddition, (3) “pearl necklace” polymers with fullerenes mutually linked covalently to form polymer chains, and (4) “charm bracelet” polymers containing pendant fullerene substituents. The methods of electrochemical polymerization of these systems are described and assessed. The structural features and properties of the electrochemically prepared polymers and their chemically synthesized analogs are compared. Polymer films containing fullerenes are electroactive in the negative potential range due to electroreduction of the fullerene moieties. Related films made with fullerenes derivatized with electron-donating moieties as building

blocks are electroactive in both the negative and positive potential range. These can be regarded as “double cables” as they exhibit both *p*- and *n*-doping properties. Fullerene-based polymers may find numerous applications. For instance, they can be used as charge-storage and energy-converting materials for batteries and photoactive units of photovoltaic cell devices, respectively. They can be also used as substrates for electrochemical sensors and biosensors. Films of the C<sub>60</sub>/Pt and C<sub>60</sub>/Pd polymers containing metallic nano-particles of platinum and palladium, respectively, effectively catalyze the hydrogenation of olefins and acetylenes. Laser ablation of electrochemically formed C<sub>60</sub>/M and C<sub>70</sub>/M polymer films (M=Pt or Ir) results in fragmentation of the fullerenes leading to the formation of hetero-fullerenes, such as [C<sub>59</sub>M]<sup>+</sup> and [C<sub>69</sub>M]<sup>+</sup>.

**Keywords** Fullerenes · Fullerene polymer films · Fullerene electropolymerization · Fullerene homopolymers · “Pearl necklace” fullerene polymers · “Charm bracelet” fullerene polymers · “Double-cable” fullerene polymers · Charge-storage fullerene polymeric materials · Catalyzed hydrogenation of olefins and acetylenes · Heterofullerenes

---

Dedicated to Professor Dr. Alan M. Bond on the occasion of his 60th birthday.

---

K. Winkler (✉)  
Institute of Chemistry, University of Białystok,  
Piłsudskiego 11/4,  
15-443 Białystok, Poland  
e-mail: winkler@uwb.edu.pl

A. L. Balch  
Department of Chemistry, University of California,  
Davis, CA 95616, USA  
e-mail: albalch@ucdavis.edu

W. Kutner  
Institute of Physical Chemistry, Polish Academy of Science,  
Kasprzaka 44/52,  
01-224 Warsaw, Poland  
e-mail: wkutner@ichf.edu.pl

## Introduction

The structure and properties of fullerenes and a large variety of fullerene derivatives provide an unprecedented diversity of macromolecular systems suitable for forming technologically promising materials [1–6]. The incorporation of the pseudo-spherical  $\pi$ -electron cages of fullerenes into solid-phase materials can significantly modify their electronic, magnetic, and optical properties.

Fullerenes can be viewed as prospective components of macromolecular and supramolecular structures. On one hand, atoms or small molecules can be trapped inside the fullerene cages [7–9], while the fullerenes or *endo*-fullerenes themselves, on the other hand, can be embedded inside large macrocycle molecules [10, 11], such as cyclodextrins [12–14], calixarenes [15–18], crown ethers [19], or porphyrins [20–22].

Fullerenes can be readily derivatized with dendrimeric macrostructures [23, 24] and covalently incorporated into macromolecular chains attached, for instance, to the porphyrin cores [25]. The significant advantage of these dendrimeric structures over parent fullerenes consists in their higher solubility [24]. Moreover,  $C_{60}$  can form a core of the star-like co-polymers with the polyacrylonitrile [26] or polystyrene [27–29] arms. The chemical and physical properties of these macromolecules can be conveniently tuned by controlling the number and length of the polymeric chains attached to the  $C_{60}$  cage.

Fullerenes are attractive as building blocks for polymers. Figure 1 shows the structural features of the three most common arrangements of fullerene-containing polymers. Fullerene homopolymers (Fig. 1a) are formed through [2+2] cycloaddition. This cycloaddition can be induced by excitation with photons [30–32], electrons [33], plasma discharge [34], or application of high hydrostatic pressure [35, 36]. Fullerene homopolymers can be also found in ambient-temperature phases of alkali metal fullerenes [37–41]. These homopolymers are relatively unstable and, therefore, have limited practical importance.

Fullerene moieties can be incorporated into other types of polymeric networks [4]. The radical “in-chain” fullerene addition leads to the formation of a “pearl necklace” structure with fullerene units forming a polymeric chain (Fig. 1b). The  $C_{60}$ -*p*-xylene co-polymer is expected to be a side-chain polymer [42]. Free-radical co-polymerization of styrene or methylmethacrylate and  $C_{60}$  is also possible [43–45]. However, the structures of the resulting polymeric materials are poorly defined.

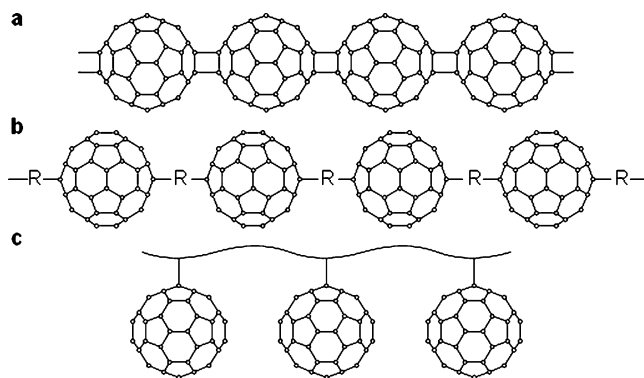


**Fig. 1** Structural features of fullerene polymers **a** homopolymer, **b** “pearl necklace”, **c** “charm bracelet” or “cherry tree branch”

The covalent incorporation of fullerene moieties into the side chains of the polymers as pendant substituents results in a “charm bracelet”, sometimes called “cherry tree branch” structure (Fig. 1c). There are at least two preparative approaches to formation of these polymers. In one, the fullerene is reacted with a pre-formed polymer, while in the other a monomer containing a fullerene as a pendant moiety is polymerized. Hydroamination is one of the most commonly used methods for grafting fullerenes onto functionalized polymeric chains [46–48]. In polymers prepared that way, a fullerene can be partially cross-linked due to multiple additions of the amine groups. Hydroamination can be enhanced by photoinduction. For instance, pendant [60]fullerene-poly(propionylethylenimine-*co*-ethylenimine) can be prepared photochemically [49]. Another method of “charm bracelet” polymer preparation involves the [2+3] cycloaddition of an azide functional group to a fullerene. This method was applied, for instance, in the preparation of pendant [60]fullerene-poly(styrylazide) [50]. The Diels–Alder cycloaddition reaction allows the incorporation of electron-deficient fullerenes into polymeric chains that bear electron-rich organic bis-dienes or aromatic moieties [51–53].

So far, chemical polymerization is mostly used for the preparation of fullerene-containing polymers. However, the rate of chemical polymerization is difficult to control. Moreover, the structure of the resulting systems is poorly defined in many cases. Using electrochemical polymerization instead can remove some of these disadvantages. Electropolymerization is a well-established method for the preparation of electroactive polymeric thin films. It allows control over not only the rate of polymerization and the structure of the resulting macromolecular system but also of the oxidation state of the polymer and the degree of polymer doping with ions of a supporting electrolyte. In addition, electropolymerization has the advantage that the polymer is directly deposited on the surface of a conducting support material. Therefore, this procedure can be readily used to construct electronic and optical devices, chemical sensors, or biosensors directly on electrodes.

The electroactivity of these polymers is affected by the presence of fullerenes in their network. Fullerenes exhibit high electron-storage capacity. For instance, both  $C_{60}$  and  $C_{70}$  are electroreduced in six reversible, one-electron steps [54]. These fullerenes can be also oxidized at relatively high positive potentials [55, 56]. After being incorporated into polymeric structures, the fullerene moieties generally retain their electrochemical activity.

The present review is focused on the electrochemical preparation and properties of polymers containing fullerene moieties. In recent years, extensive electrochemical studies have been performed on these fullerene-based polymers. Fullerene moieties have been incorporated into electro-

chemically prepared network of preformed polymers. Monomers containing fullerenes as pendant substituents were also electropolymerized. Electroreduction of  $C_{60}$  in the presence of lithium cations or electroreduction of  $C_{60}$  epoxide resulted in the deposition of polymer films on the electrode surfaces. Two-component polymer films, composed of fullerenes and transition metal complexes, have also been prepared electrochemically. These two-component polymers are the largest group of fullerene polymers synthesized electrochemically. The electropolymerization processes resulting in two-component polymers are critically reviewed herein. The prospective applications of electrochemically formed electroactive fullerene polymers are also addressed.

### Incorporation of fullerenes into electrochemically formed polymeric networks

Different polymers can be effectively doped with fullerenes or fullerene derivatives. Thick polymer films with entrapped fullerenes are typically prepared by casting solutions of these polymers onto the electrode surfaces and solvent evaporation [57–62]. Poly(3-alkylthiophene) [57] and polychlorostyrene [58] doped with  $C_{60}$  were prepared in this fashion. These polymer films are electroactive in the negative potential range due to electroreduction of the  $C_{60}$  sites.

Moreover,  $C_{60}$  can be entrapped in a polymeric matrix of polypyrrole during its polymerization [59]. For that purpose, a colloidal suspension of pyrrole and a  $C_{60}$  derivative was placed on the electrode surface and solvent was evaporated. The electropolymerization of this modified electrode was performed in an aqueous solution under potentiostatic conditions. The polymer prepared in this fashion entraps in

its network fullerenes or fullerene derivatives. The voltammetric behavior of a polypyrrole derivative, **1**, doped with the  $C_{60}$  adduct, **2**, is shown in Fig. 2. The current measured at positive potentials is due to electro-oxidation of the polypyrrole matrix. In the negative potential range, however, the fullerene sites in **2** are electroreduced.

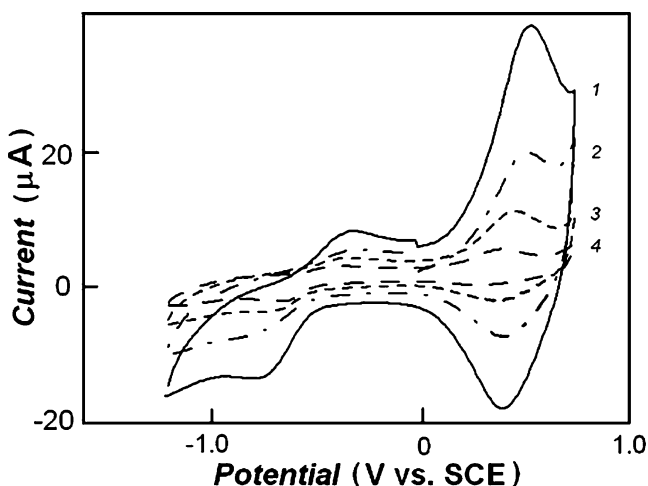
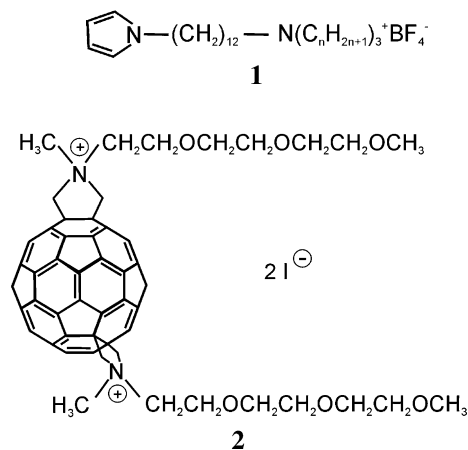


**Fig. 2** Cyclic voltammograms for a poly-1/2 film electropolymerized onto a glassy carbon electrode in 0.1 M  $\text{LiClO}_4$ . Potential scan rate was (1) 200, (2) 100, (3) 50, and (4) 20 mV/s (adapted from [59] with permission from Royal Chemical Society)

Another interesting approach to polymer doping with fullerenes involves permeation of fullerene anions through a membrane of a suitable polymer [60]. For example, a solid polyethylene film was sandwiched between a  $\text{Pt}_x\text{Li}$  alloy anode and a stainless steel cathode that was coated with a thin film of  $C_{60}$  (Fig. 3a). During electrolysis, the fullerene was electroreduced and  $C_{60}^{n-}$  anions diffused into the polyethylene matrix (Fig. 3b).

The presence of fullerenes in the polymeric network results in significant changes of the electronic properties of the host polymeric material. The electrical conductivity of the polymer can be accordingly enhanced as a result of the  $C_{60}$  doping [57, 58]. Photoconductive polymers are markedly sensitized due to this doping [57]. The photo-

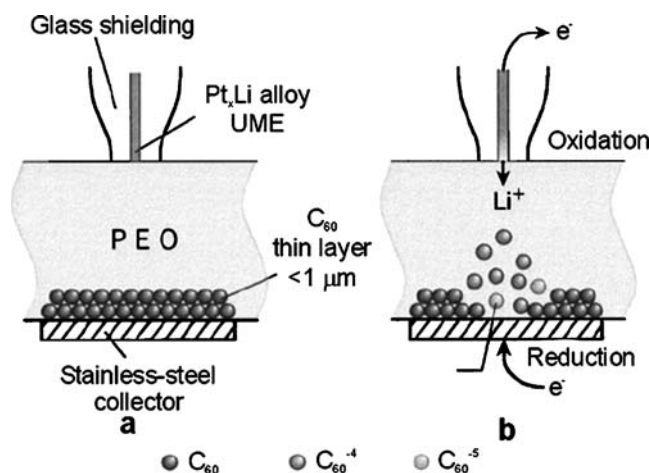
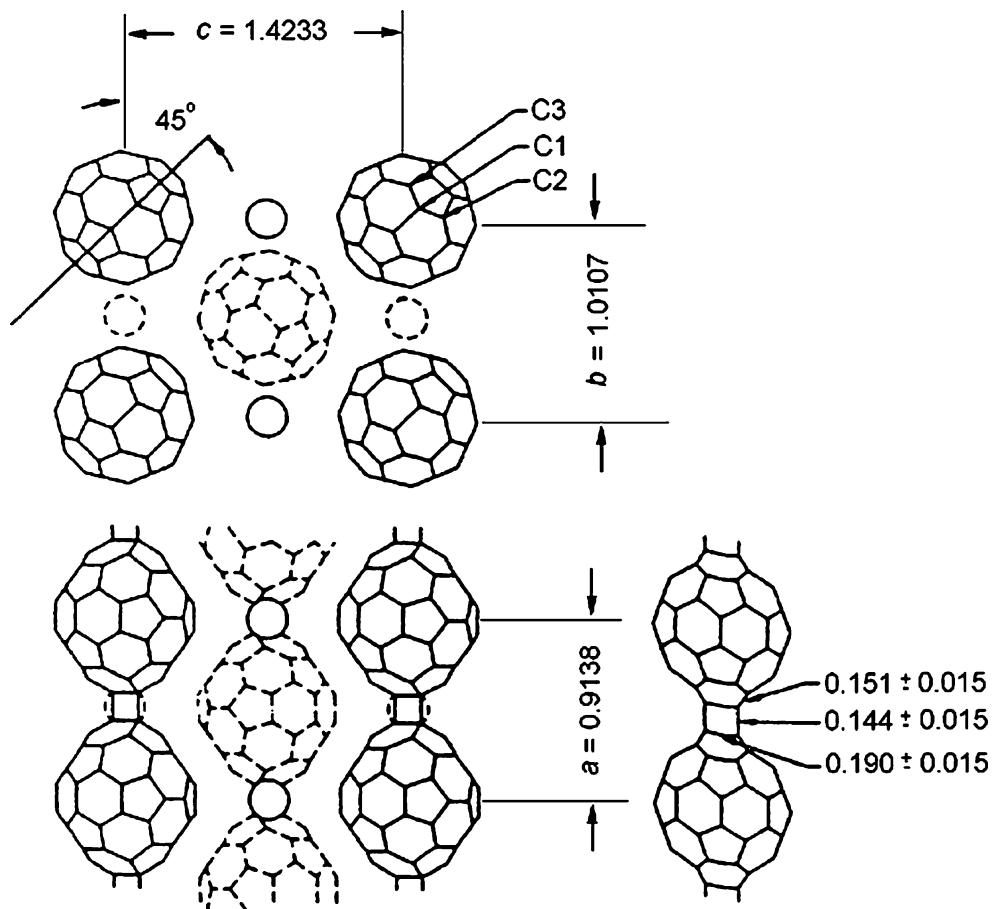


**Fig. 3** Schematic illustration of electrochemical incorporation of  $C_{60}^{n-}$  anions into a polyethylene network. **a** Initial conditions; **b** electroreductive generation of  $C_{60}^{n-}$  anions and their diffusion into the polymer film (adapted from [60])

**Fig. 4** Structural formulas of the  $(\text{RbC}_{60})_n$  polymeric chains along the  $a$  direction. *Solid (broken)* lines show fullerenes and cations centered at  $x=0$  ( $x=1/2$ ) in the  $b$ – $c$  plane at the top, and  $y=0$  ( $y=1/2$ ) in the  $a$ – $c$  plane in the bottom. The fragment to the *right* is a projection of one polymeric chain perpendicular to the  $b$ – $c$  plane. *Small circles* stand for rubidium cations. All distances are given in nanometers (adapted from [37])

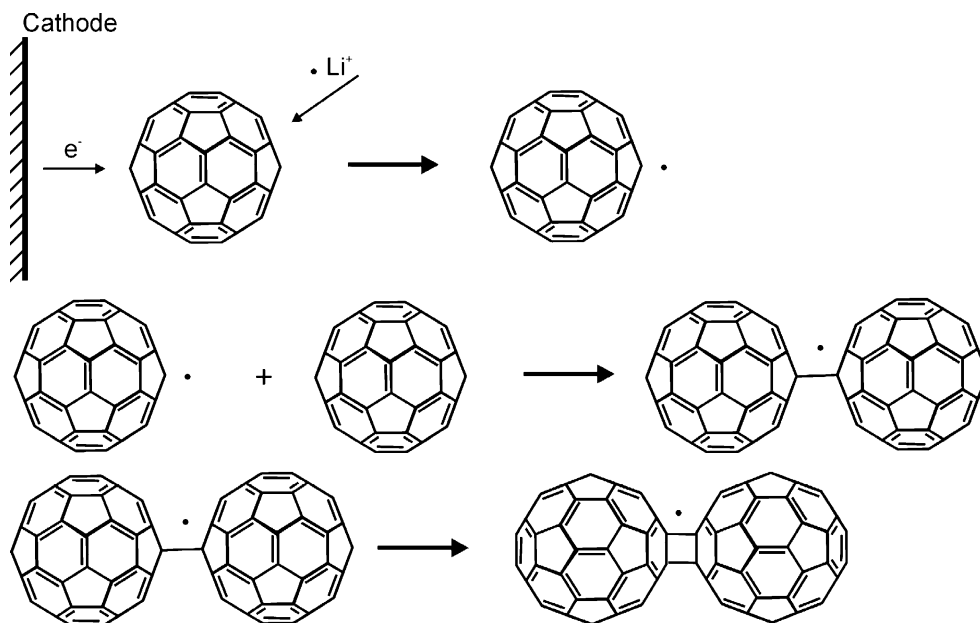


conductivity of many polymers prepared by chemical polymerization can also be enhanced due to the presence of fullerenes [61–65]. This effect is attributed to the electron transfer between the fullerene and the polymer.

#### Homopolymers of $\text{C}_{60}$ and $\text{C}_{70}$

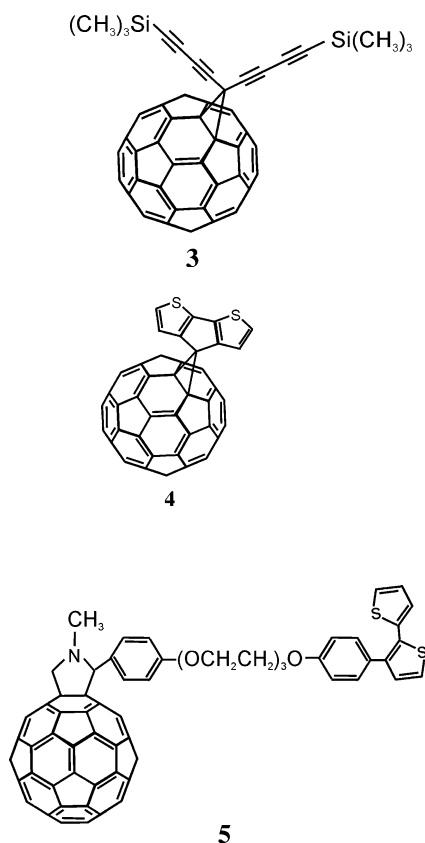
The formation of fullerene homopolymers can be induced by excitation with photons [30–32], electrons [33], plasma discharge [34], or by application of high hydrostatic

**Scheme 1**



pressure [35, 36]. The chemical formation of homopolymers was also reported for alkali metal fullerenes [37–41]. That is, a rather unusual phase transition was observed for the  $MC_{60}$  ( $M=K, Rb,$  or  $Cs$ ) fullerenes at 400 K. X-ray diffraction studies have shown that the  $RbC_{60}$  orthorhombic structure was formed with an amazingly short separation (0.91 nm) between the centers of the  $C_{60}$  cages [37]. An isostructural phase of  $KC_{60}$  was observed at ambient temperatures as well [40]. It was suggested that the  $[C_{60}]^-$  anions form a polymeric chain in the orthorhombic phase by virtue of ionically induced [2+2] cycloadditions. The structural features of the  $(RbC_{60})_n$  polymeric phase are shown in Fig. 4 [37]. In related work, it has been shown that co-crystallization of  $C_{60}$  and *p*-bromocalix[4]arene leads to formation of almost perfectly linear filaments [66] comprised of linear polymers formed via [2+2] cycloaddition with no cross-linked products.

Homopolymers of  $C_{60}$  can be also prepared by electropolymerization. The electroreduction of solutions of  $C_{60}$  and lithium salts results in deposition on the electrode surface of a negatively charged polymeric phase of  $C_{60}$  that is intercalated with  $Li^+$  counter ions, [67]. The suggested mechanism of the polymer film formation is shown in Scheme 1. In this mechanism, the ion-pair dimer,  $C_{120}^-Li^+$ , is initially formed through  $C_{60}$ . Subsequent additions of fullerene radicals to the fullerene dimer promote the growth of the polymeric phase.



The formation of homopolymers induced by electrochemically formed fullerene cations has recently been reported [68].

### Electrochemically synthesized “charm bracelet” polymers

$C_{60}$  molecules can be introduced as pendant substituents into side chains of polymers to form “charm bracelet” polymers. There are two general synthetic approaches to the formation of these systems. They involve either (1) reacting fullerene or a fullerene derivative with a pre-prepared polymer or (2) polymerizing a monomer containing a fullerene as a pendant substituent. In case of electropolymerized “charm bracelet”

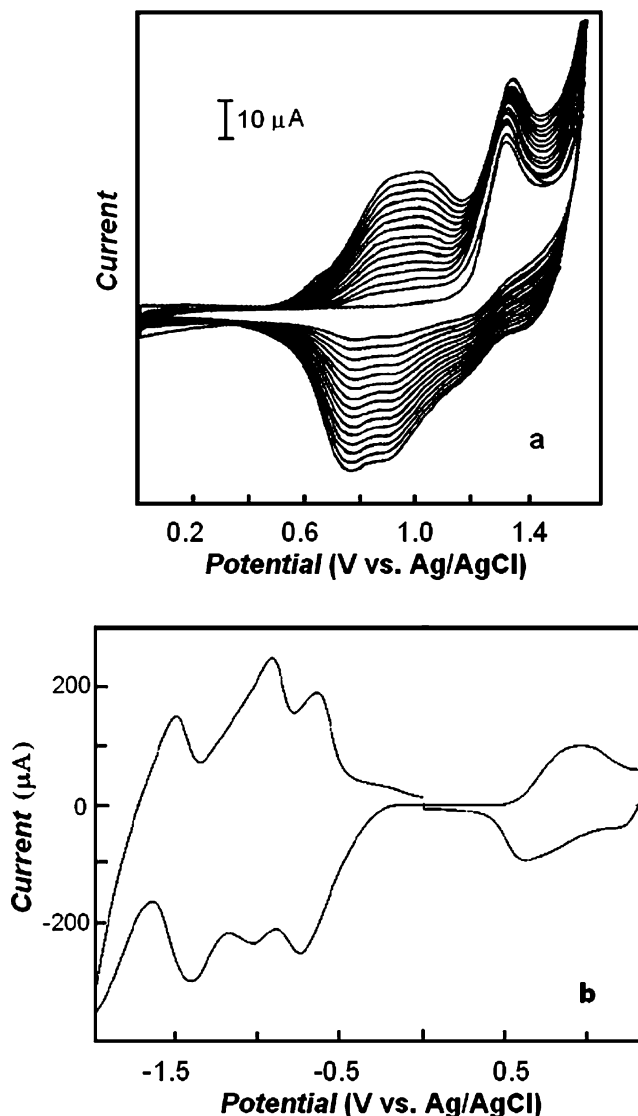


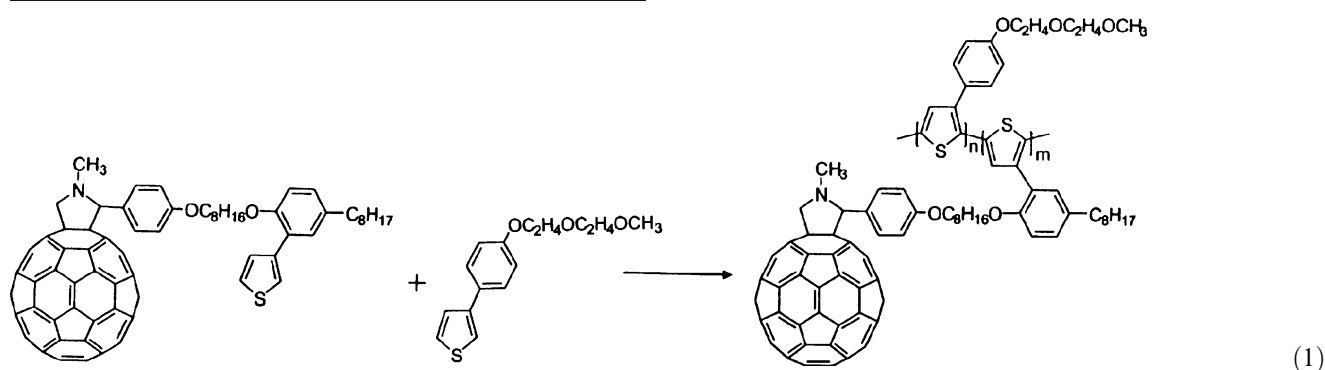
**Fig. 5** **a** Multi-scan cyclic voltammogram for **5** in 0.1 M (*n*-Bu<sub>4</sub>N)NPF<sub>6</sub>, in dichloromethane, at a Pt foil working electrode. The potential scan rate was 100 mV/s. **b** Cyclic voltammogram for a Pt foil coated by a poly-**5** film in 0.1 M (*n*-Bu<sub>4</sub>N)PF<sub>6</sub>, in dichloromethane. The potential scan rate was 100 mV/s (from [70] with permission from American Chemical Society)

polymers, the latter approach has been used. The methanefullerenes **3** and **4** as well as pyrrolidinofullerene derivative **5** have been used as precursors for this electropolymerization [69–74]. The synthesis of these precursors is a challenge by itself. Gram-quantities of the methanefullerene derivatives **3** and **4** can be prepared by using the Bigel–Hirsch method or by polar cycloaddition [75]. The Prato reaction that involves 1,3-dipolar cycloaddition of azomethine ylides to  $C_{60}$  is a convenient method of pyrrolidinofullerene synthesis [76].

Panel (a) of Fig. 5 shows a multi-scan cyclic voltammogram recorded during electrosynthesis of *poly-5*. In this procedure, the monomer **5** is electropolymerized in the positive potential range where the thiophene moiety undergoes electro-oxidation, and a film is deposited on the electrode surface. The voltammetric behavior of *poly-5* in a monomer-free solution is shown in panel (b) of Fig. 5. One

broad anodic peak related to the electro-oxidation of the polythiophene backbone is seen in the positive potential range. In the negative range, however, voltammograms show several cathodic peaks related to multiple electro-reduction of the fullerene moieties. Thus, both the polymeric thiophene backbone and pendant fullerene moieties retain their characteristic redox properties after electropolymerization. A similar behavior was observed for the *poly-3* [69] and *poly-4* [74] “charm bracelet” polymers prepared electrochemically.

Related to *poly-5*, “double cable” materials can be also prepared by chemical polymerization [77]. The formation of a fullerene–thiophene co-polymer, which can be used for fabrication of solar cells, is described by the following reaction equation:



The stability of the electrochemical behavior of electro-active polymers under the potential cycling conditions is very important, particularly from the point of view of prospective application of the polymers as rechargeable batteries. In this regard, the *poly-5* film is stable in the positive potential range. However, this film loses its electroactivity upon potential scanning in the negative potential range [70]. Both the morphological changes of the polymer, due to film loading with large supporting electrolyte counter ions, and the dissolution of the highly negatively charged material may be responsible for this behavior.

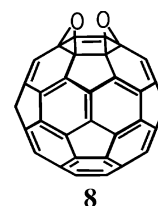
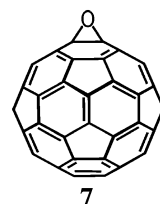
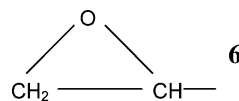
In the “charm bracelet” polymers containing fullerenes, the electron-donating backbone and the electron-accepting fullerene moieties do not interact in the ground state. However, an electron can be photoinductively transferred from the polymer backbone to the pendant fullerene moiety, for instance, in case of a polythiophene-based film [70].

### Fullerene-epoxide-based polymers

Organic compounds containing three-member epoxy ring, **6**, are used as precursors for a large group of epoxy resins. Such epoxy resins are synthesized as oligomers with the

epoxide end groups that are capable of further polymerization to form an extended polymeric network [78].

Fullerene epoxides have also been synthesized [79–81] and the structures of mono-, **7**, and bis-, **8** adducts were



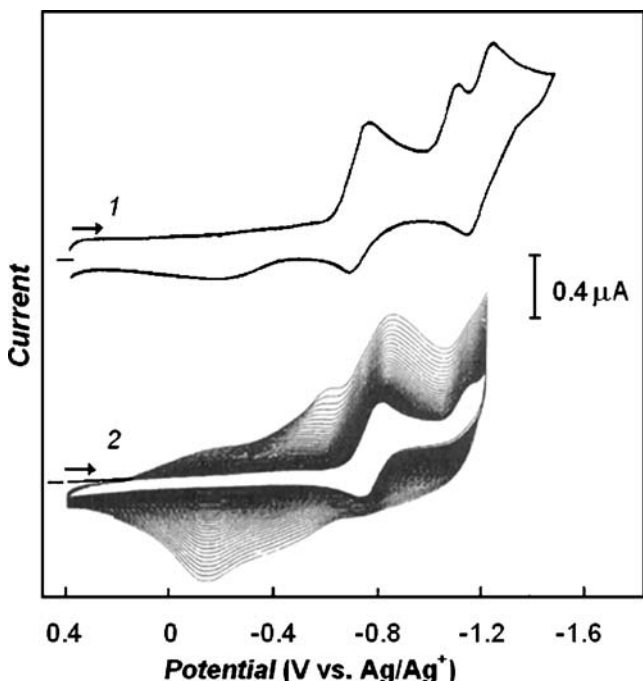
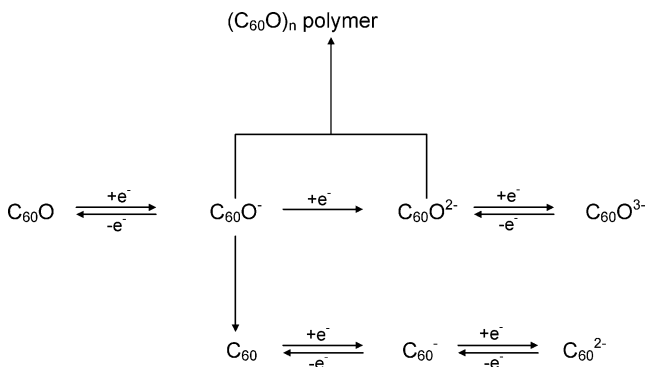


**Fig. 6** (1) Cyclic and (2) multi-scan cyclic voltammogram of 0.25 mM  $C_{60}O$  in 0.1 M  $(n\text{-Bu}_4\text{N})\text{ClO}_4$ , in an acetonitrile–toluene (1:4, v:v) mixture at the 1.5-mm-diameter Au disk electrode. The potential scan rate was 100 mV/s (adapted from [83])

determined. The fullerene epoxides,  $C_{60}O$  and  $C_{70}O$ , can be used as precursors for electrochemically induced polymerization [82, 83]. Cyclic voltammograms for  $C_{60}O$  reduction are shown in Fig. 6. The electroreduction of  $C_{60}O$  is described by the reactions in Scheme 2 [83]. The process involves the stepwise, one-electron reduction of  $C_{60}O$  followed by decomposition of the anions to form the parent  $C_{60}$  and subsequent polymerization. The product of the second electroreduction,  $C_{60}O^{2-}$ , is the crucial polymerization precursor. The rate of formation of the polymer on the electrode surface strongly depends on the nature of the solvent [83]. This effect may be attributed to the difference in solubility in different solvents of the short-chain oligomers formed at the initial stages of this electropolymerization [83].



**Scheme 2**

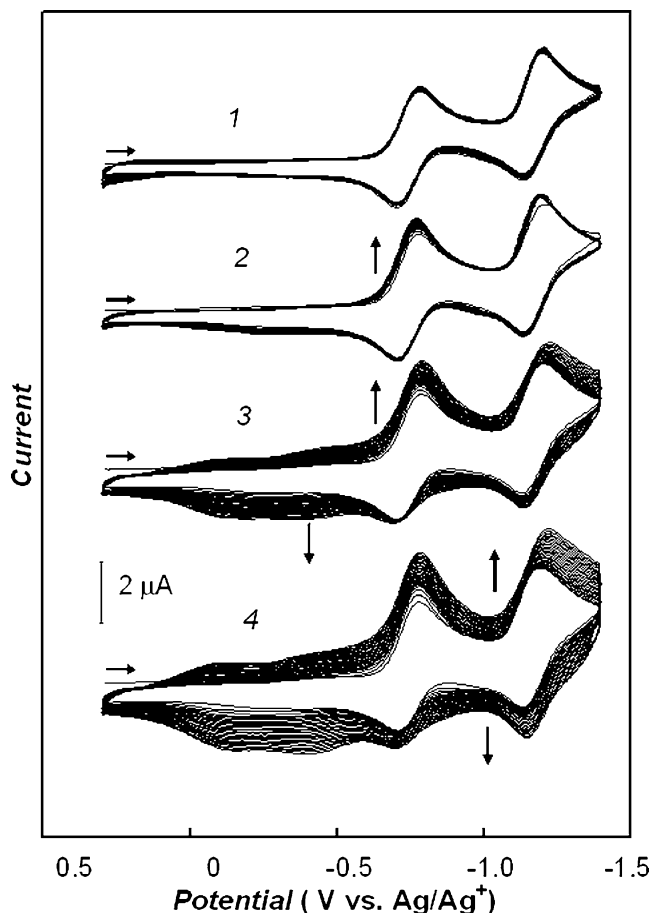
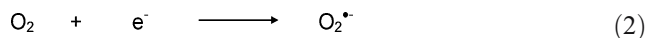
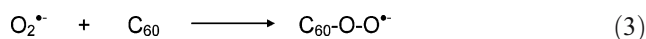


**Fig. 7** Multi-scan cyclic voltammograms at the 1.5-mm-diameter Pt disk electrode for 0.30 mM  $C_{60}$  in 0.1 M  $(n\text{-Bu}_4\text{N})\text{ClO}_4$ , in an acetonitrile–toluene (1:4, v:v) mixture, which was (1) 0, (2) 0.025, (3) 0.05, and (4) 0.11 mM in  $O_2$ . The potential scan rate was 100 mV/s (from [85] with permission from Royal Chemical Society)

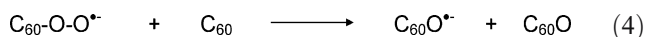
Related films can readily be prepared by electroreduction of  $C_{60}$  or  $C_{70}$  in the presence of small amounts of dioxygen in a mixed toluene–acetonitrile solution [84, 85]. Figure 7 shows multi-scan cyclic voltammograms for  $C_{60}$  in the presence of different concentrations of dissolved dioxygen. The current increase in consecutive cycles is attributed to the formation of an electroactive deposit on the electrode surface. The electrode reactions in this system are described by the sequence of reactions shown in Eqs. 2, 3 and 4. Electropolymerization is initiated here by the superoxide radical anion,  $O_2^{\cdot-}$ , which is electrogenerated at the electrode surface:



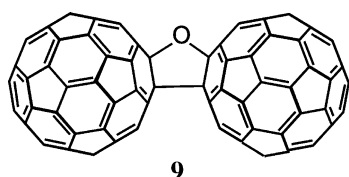
Subsequent nucleophilic addition of  $O_2^{\cdot-}$  to  $C_{60}$  may proceed within the diffuse layer at the electrode according to the following reaction equation:



A subsequent reaction of the superoxide adduct with another molecule of  $C_{60}$



may result in the formation of  $C_{60}\text{O}^{\bullet}$  and  $C_{60}\text{O}$ , which are capable of inducing further polymerization of the fullerene according to the mechanism presented in Scheme 2. X-ray photoelectron spectroscopic measurements indicated the presence of covalently bound carbon and oxygen within the film [85]. The formation of a tetrahydrofuran-like, four-membered ring like that found in the  $C_{120}\text{O}$  dimer, **9**, is particularly plausible here. Such a unit contains fragments of each reactant,  $C_{60}$ , and dioxygen. It has been established independently that  $C_{120}\text{O}$  is also formed if  $C_{60}$  is exposed to air for a prolonged time [86].



Both polymer films, i.e., that formed by electropolymerization of  $C_{60}\text{O}$  and that by electropolymerization of  $C_{60}$  in the presence of dioxygen, exhibit similar surface topography. That is, they grow to form spheroidal aggregates ranging in diameter from 0.5 to 5  $\mu\text{m}$  [84]. However, the semi-spheres grown from the fullerene and dioxygen reveal greater distribution in the grain size and are smaller than those grown from  $C_{60}\text{O}$  [84]. Two different types of topography were found for the film grown from  $C_{60}$  and  $\text{O}_2$ . One involves a relatively smooth surface of an amorphous film grown directly onto the electrode surface while the other includes polymer semi-spheres embedded within and growing out of this film. It appears that the semi-spherical aggregates of the polymer initially grow. These aggregates subsequently accrete to form a smooth, continuous film during electroreduction of a solution containing  $C_{60}$  and  $\text{O}_2$ .

Films formed from  $C_{60}\text{O}$  as well as from  $C_{60}$  and  $\text{O}_2$  retain some of their electroactivity after transfer to a blank supporting electrolyte solution (Fig. 8). However, they are unstable with respect to prolonged potential cycling. The electrochemical properties of these films depend on the nature of the supporting electrolyte present during redox cycling. The size of the counter ion consequently affects both the charge transfer rate and the conductivity of the polymer. The conductivity is lowered by the presence of larger-sized cations in the supporting electrolyte. This observation implies that the conduction currents are limited by the rate of transport of the counter cations.

The electrochemical properties of the films formed from  $C_{60}$  and  $\text{O}_2$  depend on the film thickness. That is, thick

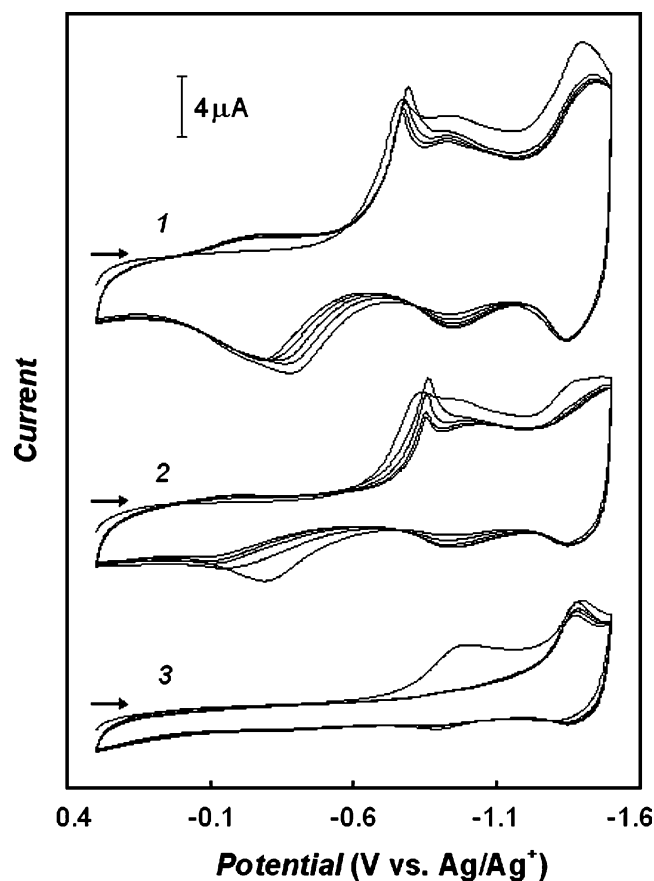


**Fig. 8** Multi-scan cyclic voltammograms at the 1.5-mm-diameter Pt disk electrode coated by a polymer film, which was electropolymerized from 0.30 mM  $C_{60}$ , 0.1 mM  $\text{O}_2$ , and 0.1 M  $(n\text{-Bu}_4\text{N})\text{ClO}_4$ , in an acetonitrile–toluene (1:4, v:v) mixture under cyclic voltammetry conditions, then transferred to a blank acetonitrile solution of (1) 0.1 M  $(\text{Et})_4\text{NClO}_4$ , (2) 0.1 M  $(n\text{-Bu}_4\text{N})\text{ClO}_4$ , and (3) 0.1 M  $(n\text{-Hx}_4\text{N})\text{ClO}_4$ . The potential scan rate was 100 mV/s (from [85] with permission from Royal Chemical Society)

films lose their electrochemical activity [87]. However, this activity may be retained in the presence of certain electroactive species in the growth solution. For instance, Fig. 9 cyclic voltammograms are shown for polymer film formation in a mixed toluene–acetonitrile solution containing  $C_{60}$ , traces of oxygen, and tetramethylphenylenediamine (TMPD). The high anodic peak current in the potential range for the tetramethylphenylenediamine electro-oxidation is related to the catalytic cycle [87] as described by Scheme 3. In this cycle, the reduced inactive form of the polymer,  $\text{poly-C}_{60}\text{O}^-$ , is chemically oxidized by the  $\text{TMPD}^+$  cation and, thus, the electrochemical activity of the film is regained. A similar behavior was observed for other electroactive species present in the polymer growth solution, such as ferrocene,  $[\text{Fe}(\text{bipyridyl})_3]^{2+}$ , or  $[\text{Ru}(\text{phenanthroline})_3]^{2+}$  [87].



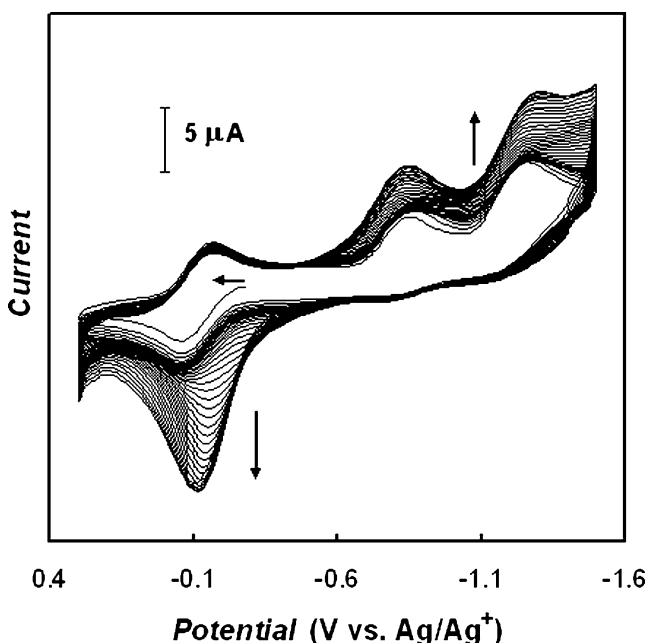


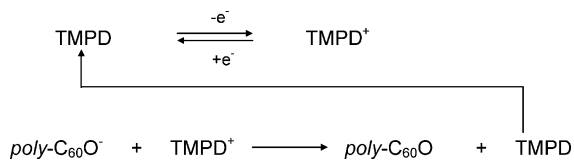
**Fig. 9** Multi-scan cyclic voltammograms at the 1.5-mm-diameter Pt disk electrode for 0.30 mM C<sub>60</sub>, 0.20 mM O<sub>2</sub>, and 0.40 mM tetramethylphenylenediamine in 0.1 M (n-Bu<sub>4</sub>N)ClO<sub>4</sub>, in an acetonitrile–toluene (1:4, v:v) mixture. The potential scan rate was 100 mV/s (from [87] with permission from Elsevier)

### Two-component films formed from fullerenes and transition metal complexes

A number of transition metal complexes has been found to add to the outer surface of fullerenes and chemically modified fullerenes [88]. This property has been exploited for preparation of polymeric chains comprised of alternating fullerenes and metal ions or complexes of metal ions. The proposed structure of this type of polymer, **10**, with the metals coordinated directly to the fullerenes in η<sup>2</sup>-fashion is shown below. In addition, cross-linking of the strands shown here may also occur in a similar way involving further η<sup>2</sup>-coordination of more metal centers.

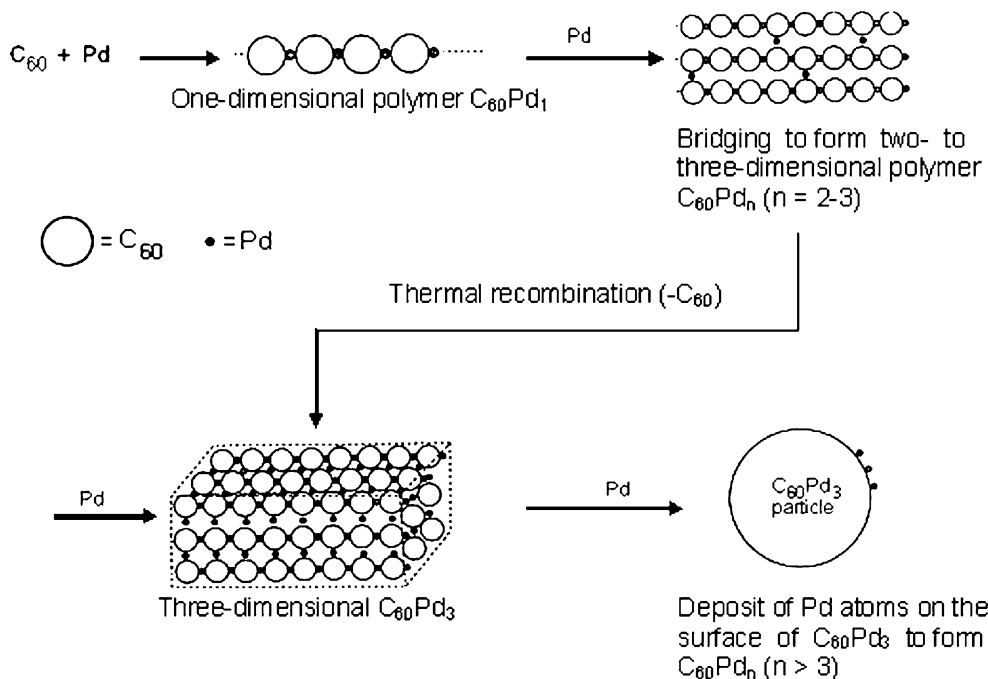
The poly-C<sub>60</sub>Pd and poly-C<sub>60</sub>Pt films were first prepared chemically by reacting C<sub>60</sub> with the palladium(0), Pd<sub>2</sub>(dba)<sub>3</sub>, or platinum(0), Pt<sub>2</sub>(dba)<sub>3</sub>, complex (dba=dibenzylideneacetone) [89–92]. The structure and the composition of these polymeric materials highly depend on the reaction stoichiometry. A schematic illustration of the formation of the poly-C<sub>60</sub>Pd<sub>n</sub> (n ranges from 1 to 7) polymer is shown in Fig. 10.

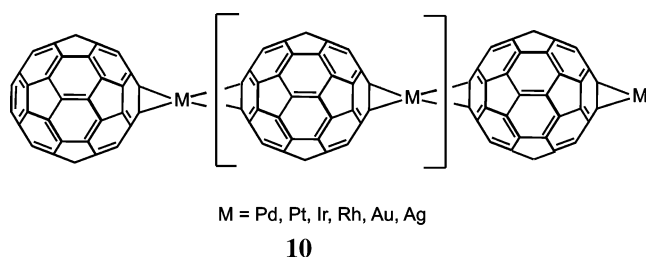
Similar polymeric materials can be prepared by reductive electropolymerization performed in an acetonitrile–toluene solution of C<sub>60</sub> and a suitable platinum(II) or palladium(II) complex. Figure 11 shows multi-scan cyclic voltammograms for the poly-C<sub>60</sub>Pd and poly-C<sub>60</sub>Pt formation. In the course of consecutive cycling in the potential range for the fullerene electroreduction, a new, solid electroactive phase is deposited onto the electrode surface. This process is accompanied by an increase in the current in the cyclic



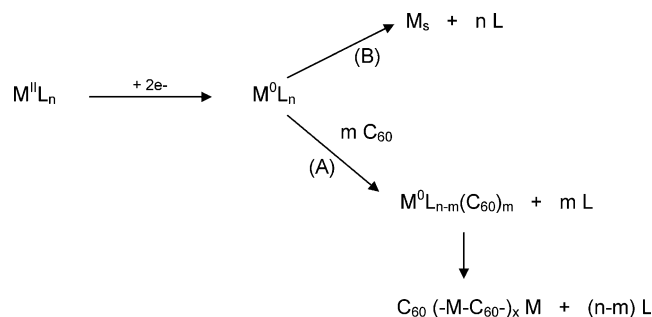
**Scheme 3**

**Fig. 10** Proposed mechanism for the chemical preparation of poly-C<sub>60</sub>Pd<sub>n</sub> (from [89] with permission from Royal Chemical Society)





voltammogram [93–95]. In case of the *poly-C<sub>60</sub>Pt* film formation, a negative shift of the electroreduction potential with the increase in the number of voltammetric scan indicates that the conductivity of this material is lower as compared to that of *poly-C<sub>60</sub>Pd*. The film formation mechanism is shown in Scheme 4 [95, 96]. Electroreduction of the Pd(II) or Pt(II) complex results in formation of the zero-valent metal intermediate,  $M^0L_n$ , and initiates the growth of the *poly-C<sub>60</sub>M* film (path A). Nanoclusters of metallic palladium or platinum,  $M_{(s)}$ , may simultaneously deposit (path B). The relative amounts of these two major products depends on the ratio of concen-



trations of precursors, i.e., the Pt(II) or Pd(II) complex and  $C_{60}$ , in the growth solution. The structure and electrochemical properties of these films markedly depend on the amount of the metallic phase that is also produced during the electroreduction process.

Related *poly-C<sub>60</sub>Rh* and *poly-C<sub>60</sub>Ir* polymer films were also prepared with the  $Rh_2(CF_3CO_2)_4$  and  $Ir(CO)_2$  units,

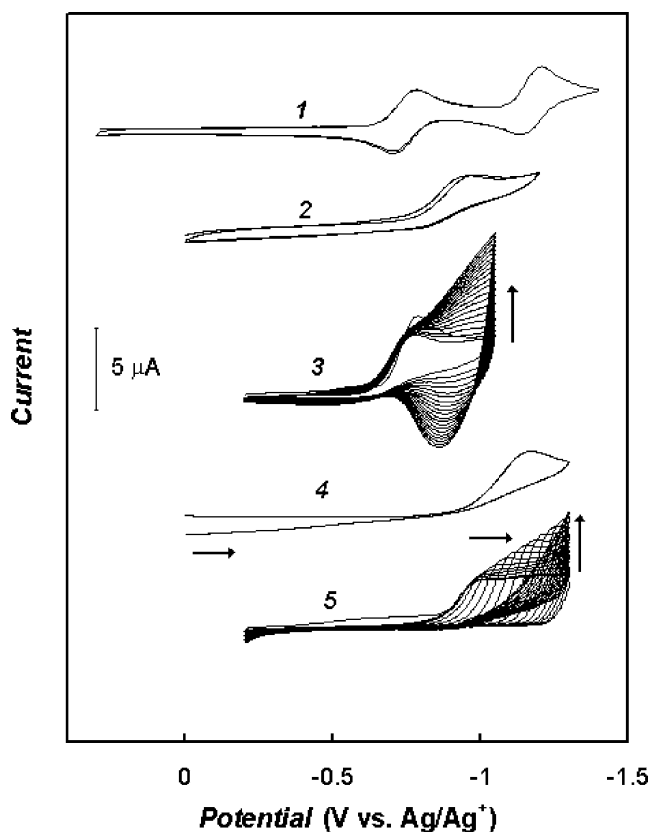


**Fig. 11** Cyclic voltammograms at the 1.5-mm-diameter Au disk electrode for (1) 0.25 mM  $C_{60}$ , (2) 2.70 mM  $Pd(CH_3CO_2)_2$ , (3) 0.25 mM  $C_{60}$  and 2.70 mM  $Pd(CH_3CO_2)_2$ , (4) 1.40 mM  $[Pt(\mu-Cl)Cl(C_2H_4)]_2$ , and (5) 0.25 mM  $C_{60}$  and 1.40 mM  $[Pt(\mu-Cl)Cl(C_2H_4)]_2$  in 0.1 M  $(n-Bu_4N)ClO_4$ , in an acetonitrile–toluene (1:4, v:v) mixture. The potential scan rate was 100 mV/s (adapted from [93, 94])

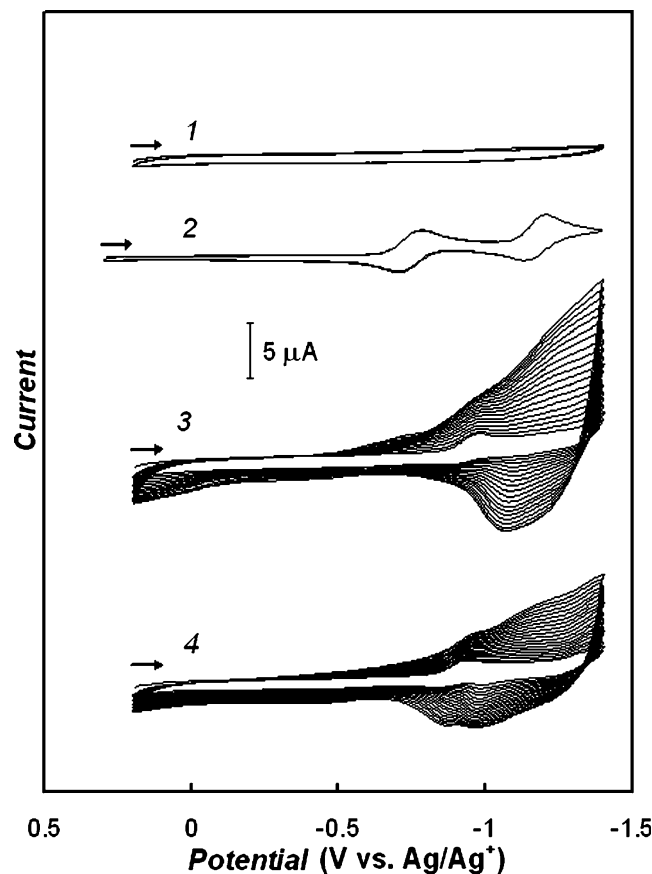


**Fig. 12** Multi-scan cyclic voltammogram at the 1.5-mm-diameter Au disk electrode for (1) 0.9 mM  $(CF_3CO_2)_4Rh_2$ , (2) 0.25 mM  $C_{60}$ , (3) 0.25 mM  $C_{60}$  and 0.85 mM  $(CF_3CO_2)_4Rh_2$ , and (4) 0.25 mM  $C_{70}$  and 0.85 mM  $(CF_3CO_2)_4Rh_2$  in 0.1 M  $(n-Bu_4N)ClO_4$ , in an acetonitrile–toluene (1:4, v:v) mixture. The potential scan rate was 100 mV/s (adapted from [93])

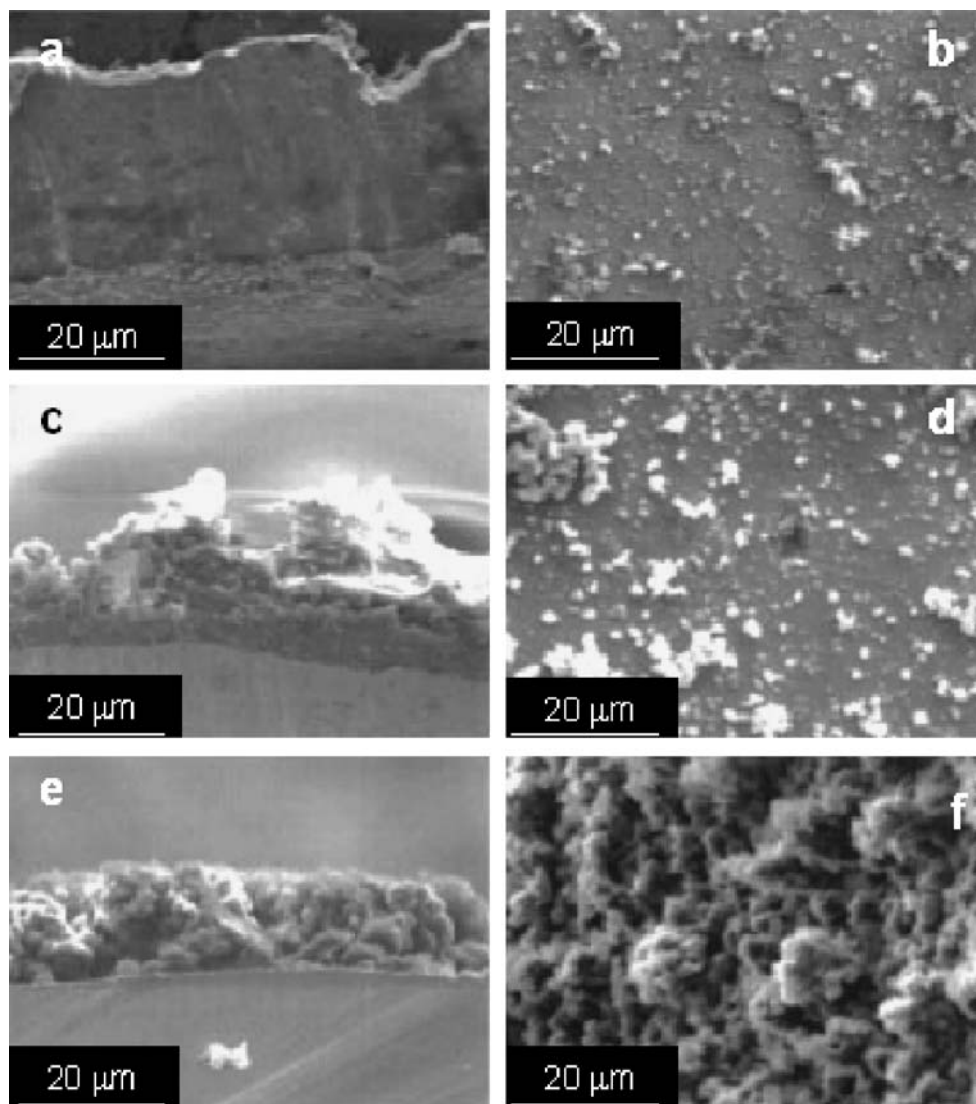
**Table 1** Precursors of electropolymerizations leading to the C<sub>60</sub>/M polymers

Polymer of C <sub>60</sub> and transition metal	Transition metal complex precursors	
C <sub>60</sub> /Pd	[Pd(CH <sub>3</sub> CO <sub>2</sub> ) <sub>2</sub> ] <sub>3</sub> Pd(CH <sub>3</sub> CO <sub>2</sub> ) <sub>2</sub>	Pd(PhCN) <sub>2</sub> Cl <sub>2</sub> <i>trans</i> -PdCl <sub>2</sub> (py) <sub>2</sub>
C <sub>60</sub> /Pt	<i>cis</i> -PtCl <sub>2</sub> (py) <sub>2</sub>	<i>trans</i> -PtCl <sub>2</sub> (py) <sub>2</sub> PtI <sub>2</sub> (py) <sub>2</sub> [Pt(μ-Cl)Cl(C <sub>2</sub> H <sub>4</sub> ) <sub>2</sub> ] <sub>2</sub>
C <sub>60</sub> /Rh	[Rh(CO) <sub>2</sub> Cl] <sub>2</sub> [Rh(CF <sub>3</sub> CO <sub>2</sub> ) <sub>2</sub> ] <sub>2</sub>	Rh(1,5-COD) <sub>2</sub> SO <sub>3</sub> CF <sub>3</sub> RhCl <sub>3</sub> (py) <sub>3</sub>
C <sub>60</sub> /Ir	[IrCl(cyclooctane) <sub>2</sub> ] <sub>2</sub>	Ir(CO) <sub>2</sub> Cl( <i>p</i> -toluidine)
C <sub>60</sub> /Au	AuCl(AsPh <sub>3</sub> )	(CH <sub>3</sub> ) <sub>2</sub> SAuCl
C <sub>60</sub> /Ag	Ag(CH <sub>3</sub> CO <sub>2</sub> )	

respectively, bridging the fullerene cages [93]. These films are also grown at negative potentials during electroreduction of C<sub>60</sub> in the presence of Ir(CO)<sub>2</sub>Cl(NH<sub>2</sub>C<sub>6</sub>H<sub>4</sub>CH<sub>3</sub>) or Rh<sub>2</sub>(O<sub>2</sub>CCF<sub>3</sub>)<sub>4</sub>. However, the iridium or rhodium complexes used as film precursors are electrochemically inactive in the potential range used for film formation. No metallic nano-particles should consequently form during

the preparation of these films. Cyclic voltammograms illustrating formation of the *poly*-C<sub>60</sub>Rh and *poly*-C<sub>70</sub>Rh films are shown in Fig. 12. The yield of the film formation was significantly different for C<sub>60</sub> and C<sub>70</sub>. The transition metal complexes that have been successfully used as precursors for electropolymerization of C<sub>60</sub> to form different *poly*-C<sub>60</sub>M films are listed in Table 1.

**Fig. 13** Scanning electron microscopy images for the film of (a, b) *poly*-C<sub>60</sub>Pd, (c, d) *poly*-C<sub>60</sub>Rh, and (e, f) *poly*-C<sub>60</sub>Ir prepared by electropolymerization. Images (a), (c), and (e) are cross-sectional views of the films on the electrode with the platinum foil electrode at the bottom. Images (b), (d), and (f) show the surface topography of the films (from [93] with permission from American Chemical Society)



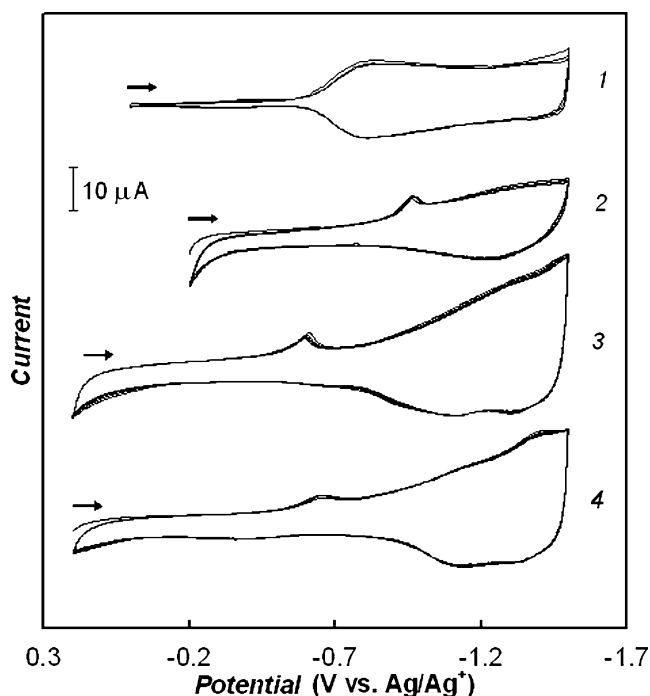


**Fig. 14** Multi-scan cyclic voltammograms at the 1.5-mm-diameter Au disk electrode coated by (1) *poly-C<sub>60</sub>Pd*, (2) *poly-C<sub>60</sub>Pt*, (3) *poly-C<sub>60</sub>Ir*, and (4) *poly-C<sub>60</sub>Rh* film in 0.1 M (*n*-Bu<sub>4</sub>N)ClO<sub>4</sub>, in acetonitrile. The potential scan rate was 100 mV/s (adapted from [93, 94])

### The structure and electrochemical properties of *poly-C<sub>60</sub>M* films

The dark-colored polymeric films, grown during electro-reduction of C<sub>60</sub> in the presence of selected transition metal complexes, strongly adhere to the surfaces of electrodes. Scanning electron microscopic images of the topography of the *poly-C<sub>60</sub>M* (M=Pd, Ir, and Rh) film surfaces are shown in Fig. 13 [93]. The surfaces of the *poly-C<sub>60</sub>Pd* and *poly-C<sub>60</sub>Ir* films are relatively smooth. The surface of the *poly-C<sub>60</sub>Rh* film is more irregular and spongy. The *poly-C<sub>60</sub>Pt* film is much more porous than the *poly-C<sub>60</sub>Pd* [94]. There are semi-spherical outcroppings on the *poly-C<sub>60</sub>Pt* film.

All these *poly-C<sub>60</sub>M* films are electroactive in the negative potential range due to the electroactivity of the fullerene moieties (Fig. 14). The film electroreduction is accompanied by ingress of the charge-compensating ions of the supporting electrolyte into the polymeric matrix. The rate of this process limits the rate of polymer electroreduction. Therefore, the rate of this electroreduction strongly depends upon the morphology of the polymer film, the nature of the supporting electrolyte, and the solvent. The cyclic voltammograms in Fig. 15 demonstrate that electroreduction of the *poly-C<sub>60</sub>Pd* and *poly-C<sub>60</sub>Pt* film depends markedly on the size of the cation of the supporting electrolyte [97]. The charge that is

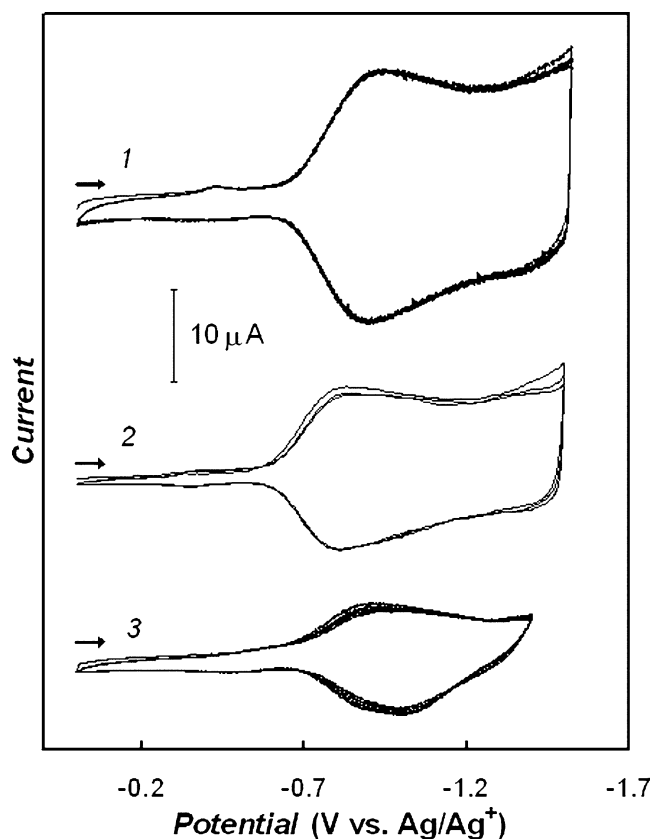
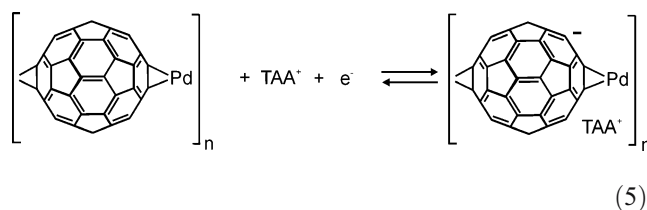


**Fig. 15** Multi-scan cyclic voltammograms at the 1.5-mm-diameter Au disk electrode coated by the *poly-C<sub>60</sub>Pd* film in (1) 0.1 M (Et)<sub>4</sub>NClO<sub>4</sub>, (2) 0.1 M (*n*-Bu<sub>4</sub>N)ClO<sub>4</sub>, and (3) 0.1 M (*n*-Hx<sub>4</sub>N)ClO<sub>4</sub>, in acetonitrile. The potential scan rate was 100 mV/s (adapted from [97])

transferred during electro-reduction and electro-oxidation of the film is higher for smaller cations. The process of film doping with cations can be described by the following equation, where TAA<sup>+</sup> is tetraalkylammonium cation [97]:



Furthermore, the voltammetric response of the *poly-C<sub>60</sub>M* films depends on the nature of the solvent [97]. The films are soluble neither in protic nor aprotic solvents. However, solvents penetrate the polymeric network and, therefore, influence the dielectric properties of the *poly-C<sub>60</sub>M* films. The ingress or egress of counter ions of the supporting electrolyte during electroreduction of the film can be also accompanied by changes in the polymer swelling with a solvent. The electrochemical properties of the *poly-C<sub>60</sub>Pd* films are consequently strongly affected by the solvent nature, as shown in Fig. 16.

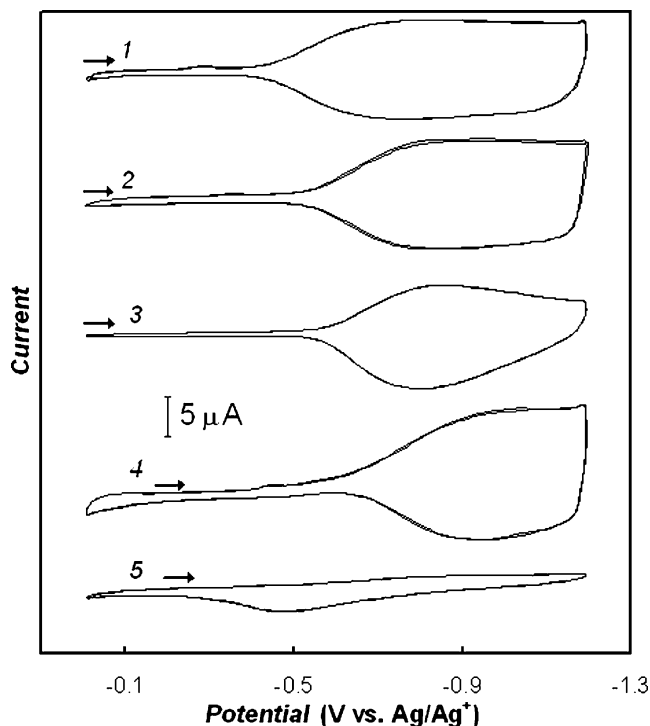


**Fig. 16** Multi-scan cyclic voltammograms at the 1.5-mm-diameter Au disk electrode coated by the *poly-C<sub>60</sub>Pd* film in (1) 0.1 M (*n*-Bu<sub>4</sub>N)ClO<sub>4</sub> in butyronitrile, (2) 0.1 M (*n*-Bu<sub>4</sub>N)ClO<sub>4</sub> in *N,N*-dimethylformamide, (3) 0.1 M (*n*-Bu<sub>4</sub>N)ClO<sub>4</sub> in propylene carbonate, (4) 0.1 M (*n*-Bu<sub>4</sub>N)ClO<sub>4</sub> in methanol, and (5) 0.1 M LiClO<sub>4</sub> in water. The potential scan rate was 100 mV/s (adapted from [97])

The conductivity of the *poly-C<sub>60</sub>M* films depends on their oxidation states. Figure 17 shows the dependence of conductivity of the *poly-C<sub>60</sub>Pd* film on potential. The data were obtained in a typical bipotentiostatic experiment performed with the use of an interdigitated microelectrode array that was coated by the film. The film is highly resistive in the potential range in which the fullerene redox centers of the polymeric network remain neutral. The electroreduction of the polymer in the negative potential range resulted in an increase in conductivity by a few orders of magnitude [93]. Moreover, this conductivity significantly depended upon the nature of counter ion present in the supporting electrolyte.

The composition of both the *poly-C<sub>60</sub>Pd* and the *poly-C<sub>60</sub>Pt* film depends upon the concentration of the film precursor in the growth solution [98, 99]. Both the metallic phase and the *poly-C<sub>60</sub>M* (M=Pd or Pt) film are deposited simultaneously from solutions containing a high concentration of either the Pd(II) or the Pt(II) complex. Cubic crystalline phases of palladium and platinum can be detected in the *poly-C<sub>60</sub>Pd* and *poly-C<sub>60</sub>Pt* films, respectively, through transmission electron microscopy. The size of the palladium and platinum nano-particles ranged from 4

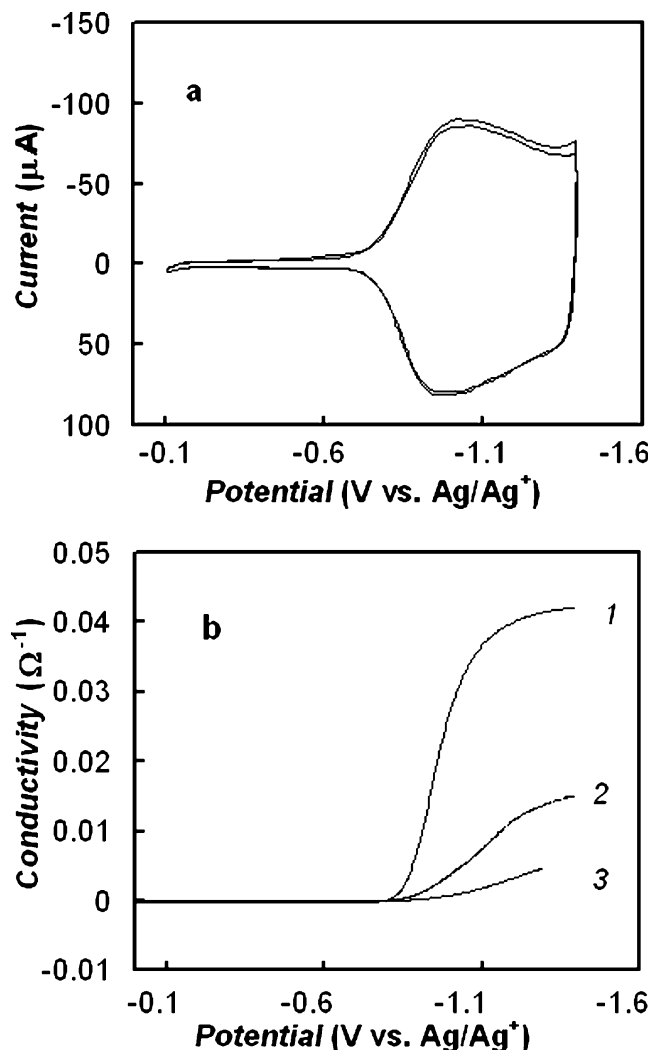


**Fig. 17** a Multi-scan cyclic voltammograms at platinum interdigitated microelectrode array coated by *poly-C<sub>60</sub>Pd* in 0.1 M (*n*-Bu<sub>4</sub>N)ClO<sub>4</sub> in acetonitrile. b Dependence of conductivity of the *poly-C<sub>60</sub>Pd* film on potential determined by using the platinum interdigitated microelectrode array in (1) 0.1 M (Et<sub>4</sub>N)ClO<sub>4</sub>, (2) 0.1 M (*n*-Bu<sub>4</sub>N)ClO<sub>4</sub>, and (3) 0.1 M (*n*-Hx<sub>4</sub>N)ClO<sub>4</sub> in acetonitrile (Winkler et al., unpublished results)

to 8 nm and 1.5 to 4 nm, respectively. Figure 18 shows an image and selected area diffraction pattern of the metallic nano-particles in the *poly-C<sub>60</sub>Pd* film [99].

The *poly-C<sub>60</sub>Pd* and *poly-C<sub>60</sub>Pt* films containing higher amounts of metallic nano-particles are less porous, compact, and more uniform. Such film morphology influences the rate of transport of the supporting electrolyte ions within the film during polymer electroreduction. The voltammetric behavior of films containing metallic nano-particles is less reversible [98]. The effects of the presence of palladium nano-particles on the electrochemical properties of the *poly-C<sub>60</sub>Pd* film are shown in Fig. 19.

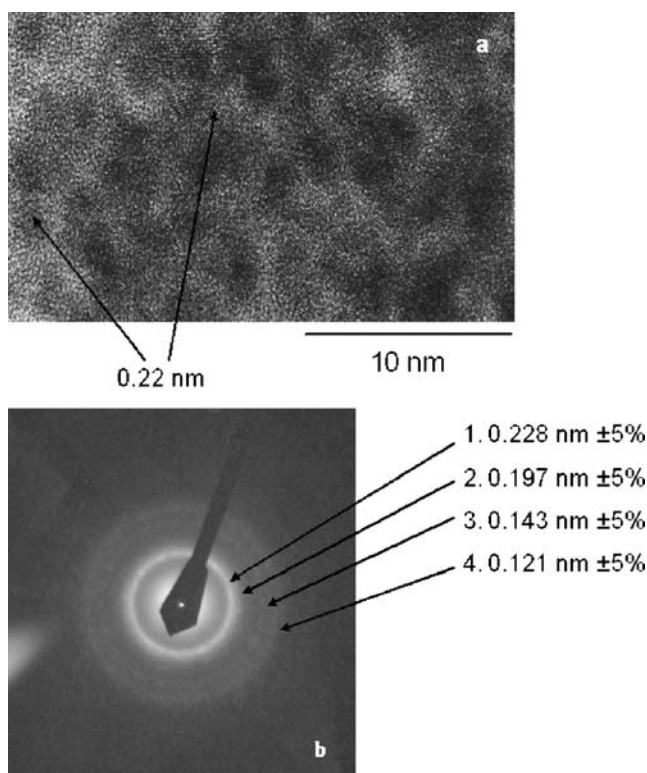


**Fig. 18** **a** High-resolution transmission electron microscopy image and **b** selected area diffraction pattern of the *poly-C*<sub>60</sub>Pd film electropolymerized on the gold foil electrode under cyclic voltammetry conditions in 0.25 mM C<sub>60</sub>, 1.25 mM [Pd(CH<sub>3</sub>CO<sub>2</sub>)<sub>2</sub>]<sub>3</sub>, and 0.1 M (*n*-Bu<sub>4</sub>N)ClO<sub>4</sub>, in an acetonitrile–toluene (1:4, v:v) mixture (from [99] with permission from Royal Chemical Society)

Metallic Pd or Pt nano-particles can effectively participate in the electron transfer. Therefore, films containing sufficient quantities of metallic nano-particles are also conductive in the potential range less negative than that required for the fullerene electroreduction.

#### “Double cables”—polymers of transition metals and fullerene derivatives

Chemically modified fullerenes can also be used as precursors for the formation of electro-active polymeric

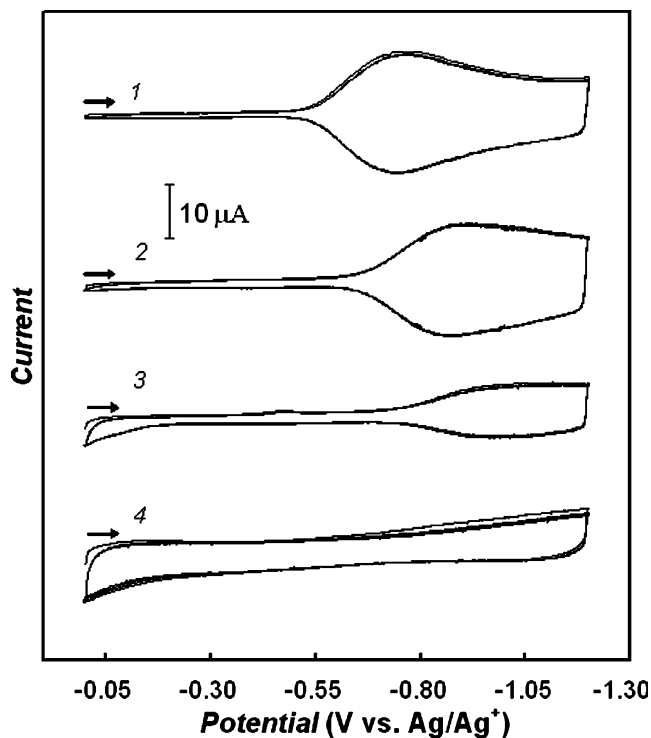
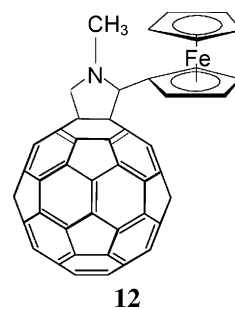
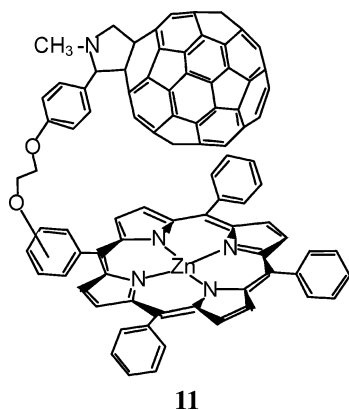
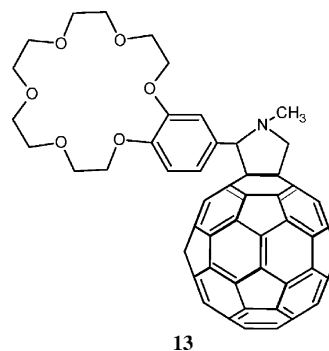


**Fig. 19** Multi-scan cyclic voltammograms at the 1.5-mm-diameter Au disk electrode coated with *poly-C*<sub>60</sub>Pd film in 0.1 M (*n*-Bu<sub>4</sub>N)ClO<sub>4</sub>, in acetonitrile. The potential scan rate was 100 mV/s. The *poly-C*<sub>60</sub>Pd films were grown under cyclic voltammetry conditions in 0.1 M (*n*-Bt<sub>4</sub>N)ClO<sub>4</sub> and (1) 0.25 mM C<sub>60</sub> and 2.25 mM Pd(CH<sub>3</sub>CO<sub>2</sub>)<sub>2</sub>, (2) 0.25 mM C<sub>60</sub> and 3.55 mM Pd(CH<sub>3</sub>CO<sub>2</sub>)<sub>2</sub>, (3) 0.25 mM C<sub>60</sub> and 6.50 mM Pd(CH<sub>3</sub>CO<sub>2</sub>)<sub>2</sub>, and (4) 0.25 mM C<sub>60</sub> and 9.35 mM Pd(CH<sub>3</sub>CO<sub>2</sub>)<sub>2</sub>, in an acetonitrile–toluene (1:4, v:v) mixture (adapted from [98])

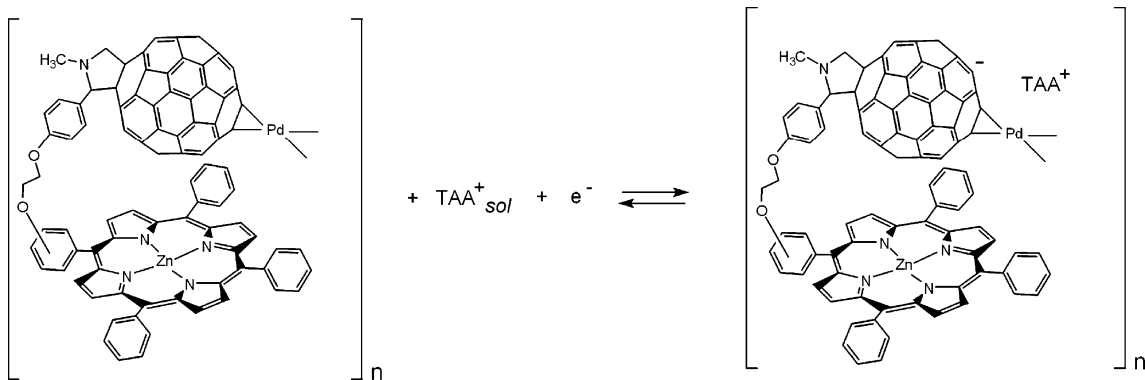


networks. For example, the structural formulae of some fullerene derivatives **11–13** used for the preparation of such polymers are shown.

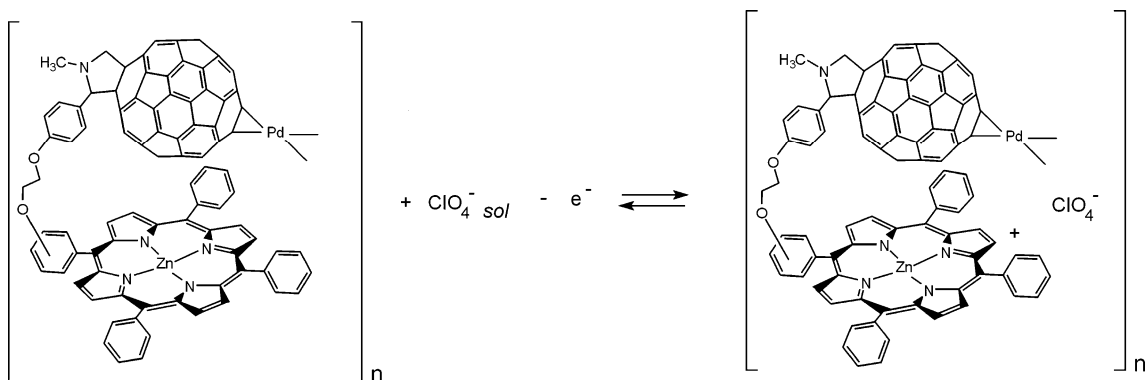
In the fullerene derivatized with zinc *meso*-tetraporphyrin (ZnPo-C<sub>60</sub> or ZnPp-C<sub>60</sub>), **11**, and the 2'-ferrocenylpyrrolidino[3',4';1,2]C<sub>60</sub>fullerene (Fc-C<sub>60</sub>), **12**, electron-donating, redox-active moieties are linked to the fullerene cages. Benzo-18-crown-6-fulleropyrrolidine (18C6-C<sub>60</sub>), **13**, can be a host for alkali metal cations.

Figure 20 shows cyclic voltammograms corresponding to electropolymerization leading to formation of the *poly*-(ZnP-C<sub>60</sub>Pd), *poly*-(Fc-C<sub>60</sub>Pd), and *poly*-(18C6-C<sub>60</sub>Pd) films [100–103]. The films were grown under similar conditions to those described above for the preparation of the *poly*-C<sub>60</sub>Pd film. The yield of formation of these films is significantly lower than that of the *poly*-C<sub>60</sub>Pd film. This is because a bulky organic moiety attached to the fullerene cage can effectively screen a large part of the fullerene moiety and make it less susceptible for reacting with the palladium complex.

Films formed from fullerenes derivatized with electron donors, like *poly*-(Fc-C<sub>60</sub>Pd) and *poly*-(ZnP-C<sub>60</sub>Pd), are electroactive both in the negative and the positive potential range [100–103]. However, the polymer films based on the crown ether derivative, **13**, are electroactive only at negative potentials. In Fig. 21, the voltammetric behavior of these films in an acetonitrile solution containing only the supporting electrolyte is shown. Broad cathodic peaks in the negative potential range correspond to the fullerene-involved electroreduction processes. This film behavior resembles that of typical  $\pi$ -conducting polymers, such as polypyrrole [104, 105], polyaniline [106, 107], and polythiophene [108–110]. The film electroreduction rate depends on the structure of the fullerene derivative. In the negative potential range, the *poly*-(ZnP-C<sub>60</sub>Pd) film reveals the most reversible behavior. The two reversible cathodic peaks observed in this range are related to two electroreductions of the fullerene moiety, according to the following reaction equations:



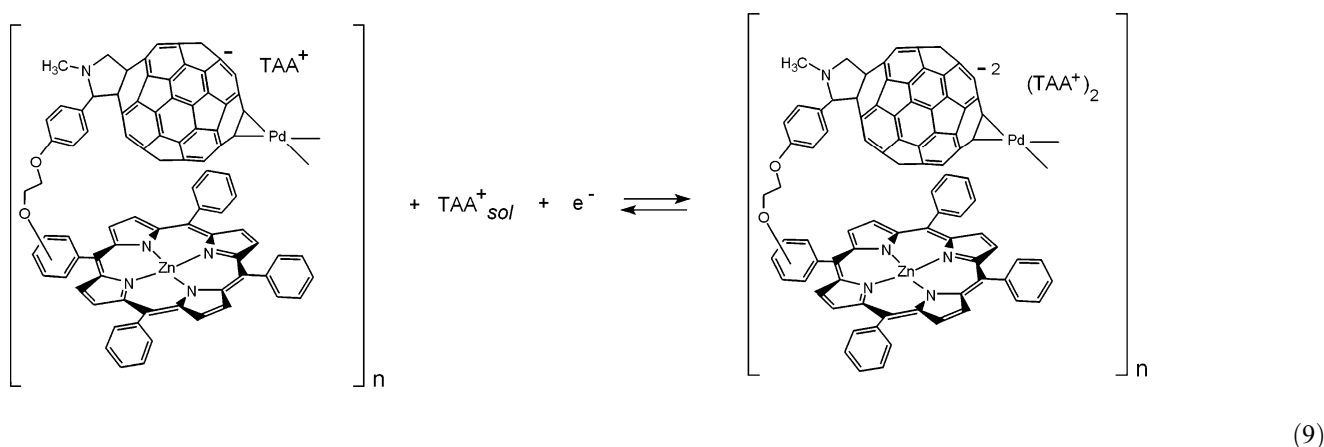
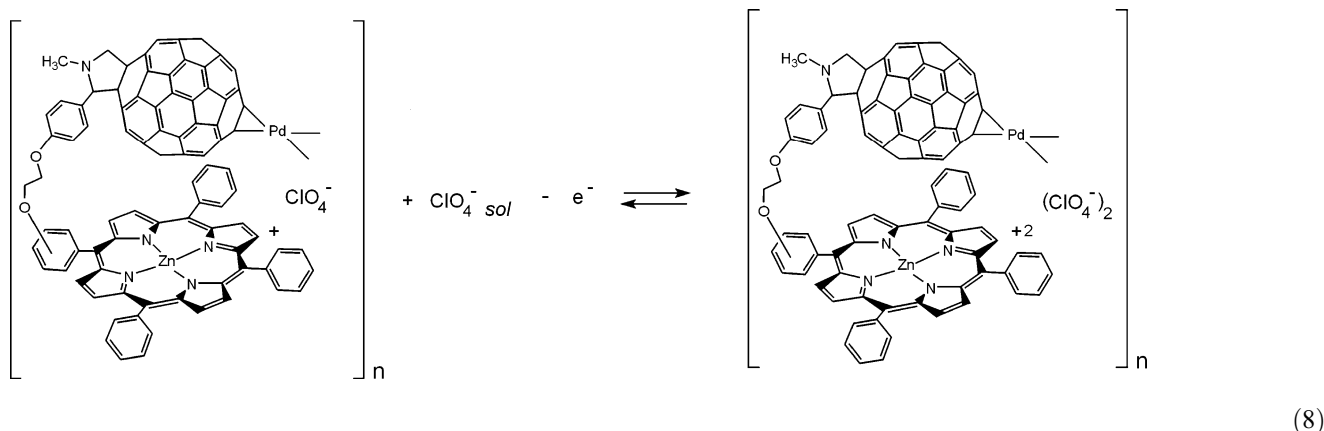
(6)



(7)

The electrode processes in the positive potential range are related to electro-oxidation of the ferrocene or zinc porphyrin

moieties. Two electro-oxidations of *poly*-(ZnP-C<sub>60</sub>Pd) can be described by the following reaction equations:



In contrast to the cathodic peaks corresponding to the electroreduction of the fullerene moieties, the anodic peaks of electro-oxidation of the ferrocene or zinc porphyrin moiety are relatively sharp and symmetrical. Moreover, the changes in the charging current associated with electro-oxidation of the film are much smaller. This behavior resembles that observed for redox polymers [111] and features charge transfer via sequential electron exchange between neighboring redox centers and, in the present case, between the ferrocene or zinc porphyrin sites as well.

#### Application of the fullerene-based, electrochemically formed polymers

Electrochemically prepared films of polymers built from fullerenes or their derivatives reveal a number of potential applications. They may be used as charge-storage materials for batteries and for photosensitive units in photovoltaic cells. Films of *poly*-C<sub>60</sub>O and “charm bracelet” polymers, such as [C<sub>60</sub>]fullerene-poly(*N*-vinylcarbazole) and [C<sub>60</sub>]fullerene-

polystyrene, may be useful for lithium secondary batteries [112]. The *poly*-C<sub>60</sub>O film appeared to be best suited as the negative electrode material among studied polymers. This polymer can be reversibly doped with lithium cations. Moreover, it is quite stable in a wide potential range and highly charge efficient in the charging–discharging cycles. The capacity of the *poly*-C<sub>60</sub>O film is very high with up to eight electrons stored per fullerene unit [112].

The polymers prepared by simultaneous electroreduction of fullerenes and transition metal complexes can be considered as promising electroactive materials for batteries. Favorable features include appreciable stability over a wide potential range, high conductivity, and high capacitance. The voltammetric behavior of the *poly*-C<sub>60</sub>Pd film in different potential ranges is shown in Fig. 22. Similar results were obtained for the *poly*-C<sub>60</sub>Pt film [94]. Both of these films retain their redox activity in the course of prolonged potential cycling in a relatively wide potential range. The decomposition of the film at potentials more negative than ca. -2.10 V vs the ferrocene/ferrocenium couple is due to strong mutual repulsions between the



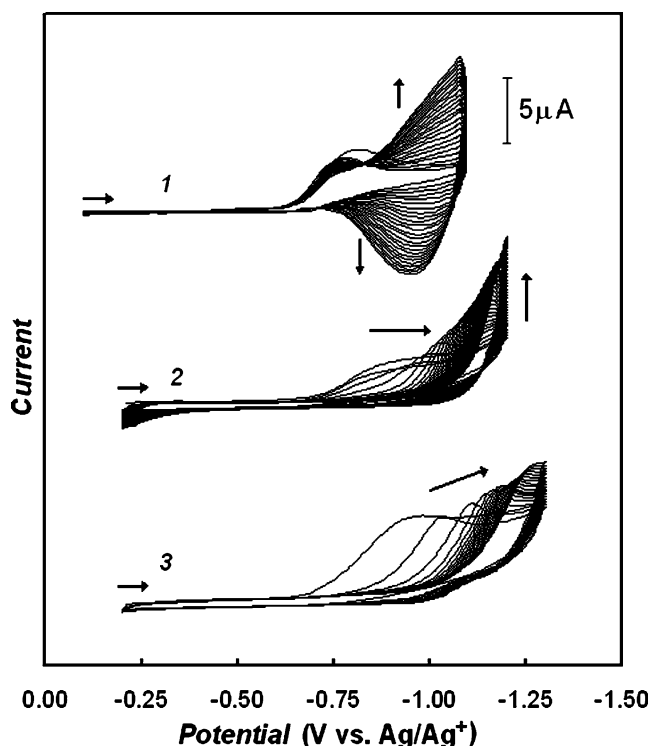


**Fig. 20** Multi-scan cyclic voltammograms at the 1.5-mm-diameter Au disk electrode for 2.70 mM Pd(CH<sub>3</sub>CO<sub>2</sub>)<sub>2</sub> and (1) 0.25 mM Fc-C<sub>60</sub>, (2) 0.30 mM ZnPo-C<sub>60</sub>, and (3) 0.25 mM 18C6-C<sub>60</sub> in 0.1 M (*n*-Bu<sub>4</sub>N)ClO<sub>4</sub>, in an acetonitrile–toluene (1:4, v:v) mixture. The potential scan rate was 100 mV/s (adapted from [100, 103])

multi-negatively charged C<sub>60</sub> sites and to mechanical strain imposed by the counter ions that entered the polymer during its electroreduction. Therefore, the potential range in which the film is stable depends mainly on the size of cation of the supporting electrolyte. The composition of the growth solution also affects the film stability through its effect on the film structure [98].

For polymers electrodeposited from solutions containing fullerenes and complexes of transition metals, the capacitance properties make them also very promising as materials for applications in electrochemical technology. For instance, in the case of the *poly*-C<sub>60</sub>Pd and *poly*-C<sub>60</sub>Pt films, two types of capacitors are conceivable:

- (1) A pseudocapacitor, which is formed in the growth solution with a relatively low concentration ratio of the palladium or platinum complex to C<sub>60</sub>.
- (2) A double-layer capacitor, which is prepared by electropolymerization from a growth solution containing a large excess of the palladium or platinum complex. The resulting film contains a large amount of the palladium or platinum nano-particles, respectively.

The values of the specific capacitance, i.e., the charge stored per mass unit, determined from the cyclic voltammograms for *poly*-C<sub>60</sub>Pd are compiled in Table 2. In general,

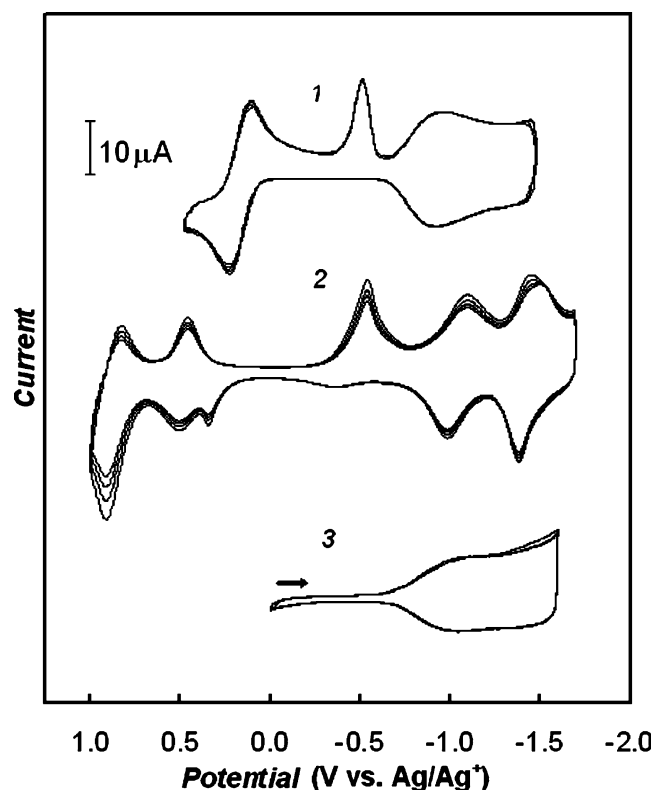


**Fig. 21** Multi-scan cyclic voltammograms for the 1.5-mm-diameter Au disk electrode coated by a film of (1) *poly*-(Fc-C<sub>60</sub>Pd), (2) *poly*-(ZnPo-C<sub>60</sub>Pd), and (3) *poly*-(18C6-C<sub>60</sub>Pd) in a 0.1 M (*n*-Bu<sub>4</sub>N)ClO<sub>4</sub> acetonitrile solution. The potential scan rate was 100 mV/s (adapted from [100, 103])

the specific pseudocapacitance depends on the size of the cation of the supporting electrolyte. The capacitance of a polymer containing a large amount of metallic palladium nanocrystals is almost independent of the solution composition used for its preparation. The high values of the specific pseudocapacitance of *poly*-C<sub>60</sub>Pd make this polymer a very attractive candidate as an active material for charge-storage devices. The specific capacitance of films containing metallic palladium is in the range of the specific capacitance of typical double-layer capacitors [113].

The presence of fullerene moieties in a conjugated polymer network may significantly increase its photoconductivity. This effect is attributed to the electron transfer between electron-donating moieties forming the polymer network and the electron-accepting fullerene sites. This photoinduced charge separation is followed by transport of the positive charge carriers to the surface of the electrode substrate through the conduction band of the conjugated polymer on one hand and transport of electrons by self-exchange between neighboring fullerene sites on the other. This effect was observed both for systems with fullerene entrapped in a polymer matrix [57, 61–65] and for a “charm bracelet” polymer of polythiophene containing a fullerene

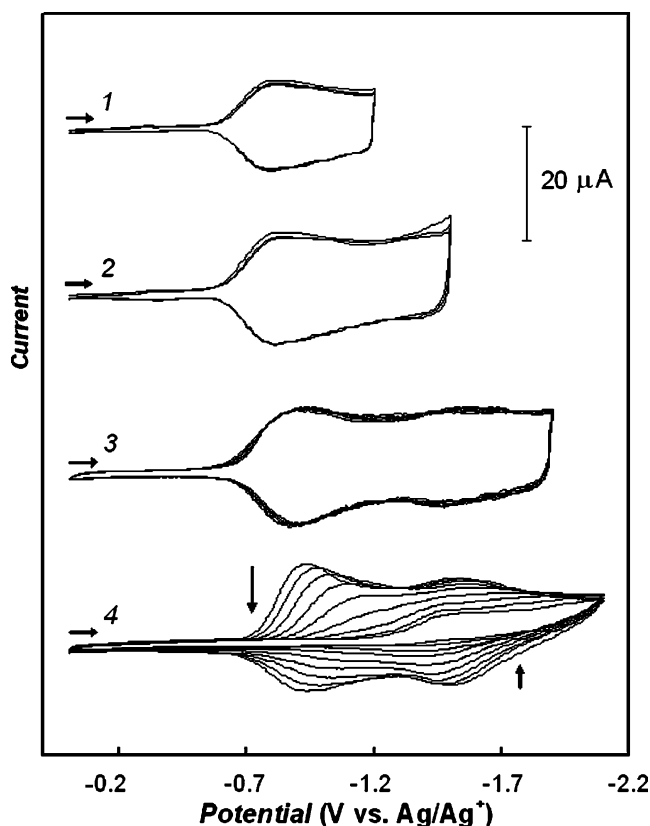


**Fig. 22** Multi-scan cyclic voltammograms for the 1.5-mm-diameter Au disk electrode coated with the *poly*-C<sub>60</sub>Pd film in a 0.1 M (*n*-Bu<sub>4</sub>N)ClO<sub>4</sub> acetonitrile solution, for the potential range (1) 0 to -1.2 V, (2) 0 to -1.5 V, (3) 0 to -1.9 V, and (4) 0 to -2.1 V. The potential scan rate was 100 mV/s (adapted from [97])

as a pendant substituent [69]. The Langmuir–Blodgett bilayer films, structured of a porphyrin–fullerene or phytychlorin–fullerene donor–acceptor dyad layer and a layer of a *poly*(3-hexylthiophene) conducting polymer, were also used for study interlayer vectorial photoinduced electron

**Table 2** Specific capacitance of the *poly*-C<sub>60</sub>Pd films in acetonitrile solutions of different tetra(*n*-alkyl)ammonium perchlorates

Supporting electrolyte	Specific capacitance (F/g)	
( <i>n</i> -Hx) <sub>4</sub> NClO <sub>4</sub>	160 <sup>a</sup>	49 <sup>b</sup>
( <i>n</i> -Bu) <sub>4</sub> NClO <sub>4</sub>	195 <sup>a</sup>	53 <sup>b</sup>
(Et) <sub>4</sub> NClO <sub>4</sub>	255 <sup>a</sup>	57 <sup>b</sup>
(Me) <sub>4</sub> NClO <sub>4</sub>	310 <sup>a</sup>	

<sup>a</sup>Polymer film electrochemically synthesized in 0.1 M tetra(*n*-butyl) ammonium perchlorate, 0.27 mM C<sub>60</sub>, and 3.6 mM Pd(CH<sub>3</sub>CO<sub>2</sub>)<sub>2</sub>, in an acetonitrile–toluene (1:4, v:v) mixture. The specific capacitance was determined from voltammograms recorded in the potential range -0.80 to -1.50 V vs ferrocene/ferrocenium

<sup>b</sup>Polymer film, rich in Pd nano-particles, electrochemically synthesized in 0.10 M tetra(*n*-butyl)ammonium perchlorate, 0.27 mM C<sub>60</sub>, and 8.9 mM Pd(CH<sub>3</sub>CO<sub>2</sub>)<sub>2</sub>, in an acetonitrile–toluene (1:4, v:v) mixture. The specific capacitance was determined from voltammograms recorded in the potential range 0 to -0.70 V vs ferrocene/ferrocenium

transfer [114, 115]. The yield of charge separation in these systems is close to unity and its lifetime is as long as a second. These photoconductive systems are promising for constructing photovoltaic devices applicable in plastic solar cells or photodetectors [116, 117].

The C<sub>60</sub> and C<sub>70</sub> fullerenes can be used as electron mediators, because they exhibit six reversible, one-electron electroreduction steps. However, poor solubilities of fullerenes and their derivatives in aqueous solutions prevent their application as diffusional electron mediators or electrocatalysts. Nevertheless, C<sub>60</sub> and its derivatives can be used as heterogeneous bioelectrocatalysts [118]. For instance, a carboxylic derivative of C<sub>60</sub> immobilized on a monolayer film of cystamine [119] and C<sub>60</sub> immobilized by adsorption onto a porous carbon electrode [120] have been used as amperometric glucose biosensors. Furthermore, fullerenes incorporated into a film of a cationic surfactant catalyzes electroreduction of hemoglobin [121]. In addition, C<sub>60</sub> embedded in a supported bilayer lipid membrane acts as an electron mediator and, therefore, can be used as an electrochemical biosensor [122]. However, these membrane systems exhibit relatively poor mechanical stability and low density of the fullerene electroactive sites. These disadvantages can be circumvented if polymeric fullerene materials are applied instead. A polypyrrole film with incorporated fullerene derivative **2** and glutathione reductase, *poly*-1/2/GR, was accordingly used as a biosensor for amperometric detection of glutathione [59]. The analytical performance of

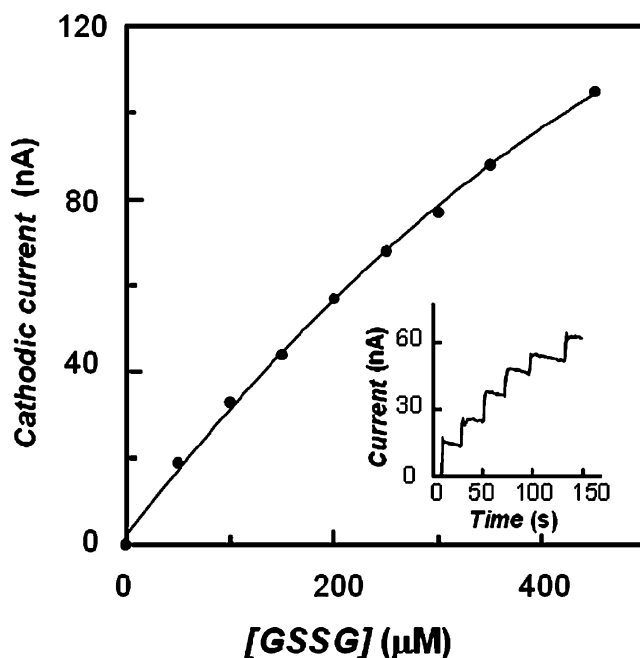
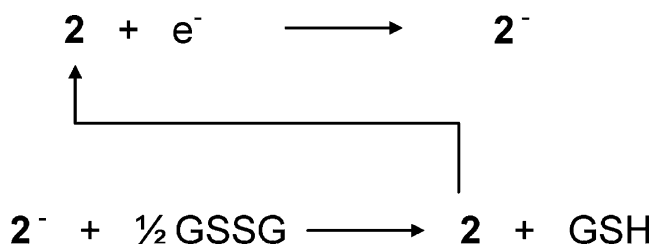


**Fig. 23** Calibration curve for glutathione determination at an electrode coated by the *poly*-1/2/GR film. Inset shows current–time curve recorded after successive additions of 50- $\mu$ M samples of glutathione in 0.1 M *N*-(2-hydroxyethyl)piperazine-*N'*-(ethane-2-sulfonic acid) (from [59] with permission from Royal Chemical Society)



Scheme 5

this sensor in the glutathione determination is shown in Fig. 23. The current measured is related to the following catalytic cycle (Scheme 5): where GSSG and GSH stand for oxidized and reduced glutathione, respectively. The response to glutathione of this *poly-1/2/GR* biosensor is fast and reproducible. Moreover, its linear concentration range is wider than those of similar devices based on diffusional redox mediators.

A *poly-C<sub>60</sub>Pd*-film-coated electrode was used to catalyze cytochrome *c* electroreduction [123]. The adsorption of cytochrome *c* on the surface of a relatively porous polymeric film is responsible for the observed bioelectrocatalytic effect. A schematic representation of the cytochrome *c* reduction at an electrode coated with the *poly-C<sub>60</sub>Pd* film is shown in Fig. 24.

The *poly-C<sub>60</sub>Pd* film can also be used for detection of carbon monoxide or imidazole (Winkler and Balch, unpublished data). As seen in Fig. 25, the voltammetric response of an electrode coated with the *poly-C<sub>60</sub>Pd* film becomes more reversible in the presence of CO, and the cathodic peak potential of the film electroreduction shifts toward less negative values. These changes in the electrochemical response of the film are presumably related to the coordination of carbon monoxide to the palladium sites within the polymer. The film formed from palladium and benzo-18-crown-6-fulleropyrrolidine, **13**, synthesized recently under electrochemical conditions (Winkler et al., unpublished

data), and related polymers of fulleropyrrolidine bearing other covalently attached crown ethers can be used for constructing electrochemical sensors for alkali metal cations.

Chemically synthesized *poly-C<sub>60</sub>Pd* was used as a catalyst for hydrogenation of olefins and acetylenes [124, 125]. Similar catalytic properties can be envisioned for the electrochemically synthesized *poly-C<sub>60</sub>Pd* and *poly-C<sub>60</sub>Pt* films containing a large amount of palladium and platinum nano-particles, respectively. The catalytic activities of these materials depend on their composition. It appeared that only the polymer containing metallic palladium nano-particles could effectively catalyze the hydrogenation of olefins and acetylenes at room temperature under a hydrogen atmosphere. An increase of the content of the metallic phase in the polymer results in an increase in the hydrogenation rate [124]. The results obtained for catalytic hydrogenation of diphenylacetylene with the use of *poly-C<sub>60</sub>Pd* catalyst with different content of Pd nano-particles are summarized in Table 3. Examples of hydrogenations catalyzed by metallic palladium nano-particles incorporated into the *poly-C<sub>60</sub>Pd* film are shown in Table 4.

The *poly-C<sub>60</sub>Pd* and *poly-C<sub>60</sub>Pt* films have also been used as very effective absorbents of gases containing a benzene ring [126]. The absorptive properties of these films with respect to vapors of toluene and other organic solvents containing this ring depend on the film composition. Among the *poly-C<sub>60</sub>Pd<sub>n</sub>* materials, the *poly-C<sub>60</sub>Pd<sub>2</sub>* film exhibits the highest absorptivity. This favorable performance is presumably related to interactions between  $\pi$ -orbitals of toluene and palladium atoms.

Laser ablation of the electrochemically synthesized *poly-C<sub>60</sub>M* and *poly-C<sub>70</sub>M* films [M=Pt or Ir(CO)<sub>2</sub>] results in fullerene fragmentation and formation of the heterofullerenes, such as C<sub>59</sub>M<sup>+</sup> and C<sub>58</sub>M<sup>-</sup> [127–129]. The structures of these novel heterofullerenes with metal sites incorporated into the carbon cage networks have been explored by computational procedures using density functional theory. Figure 26 shows

**Fig. 24** Proposed mechanism of cytochrome *c* immobilization and electroreduction at a *poly-C<sub>60</sub>Pd*-film-coated electrode (from [123] with permission from Elsevier)

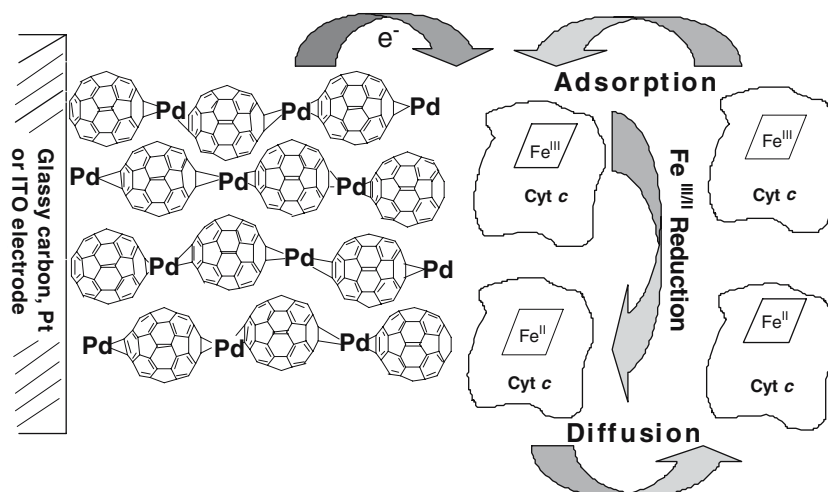
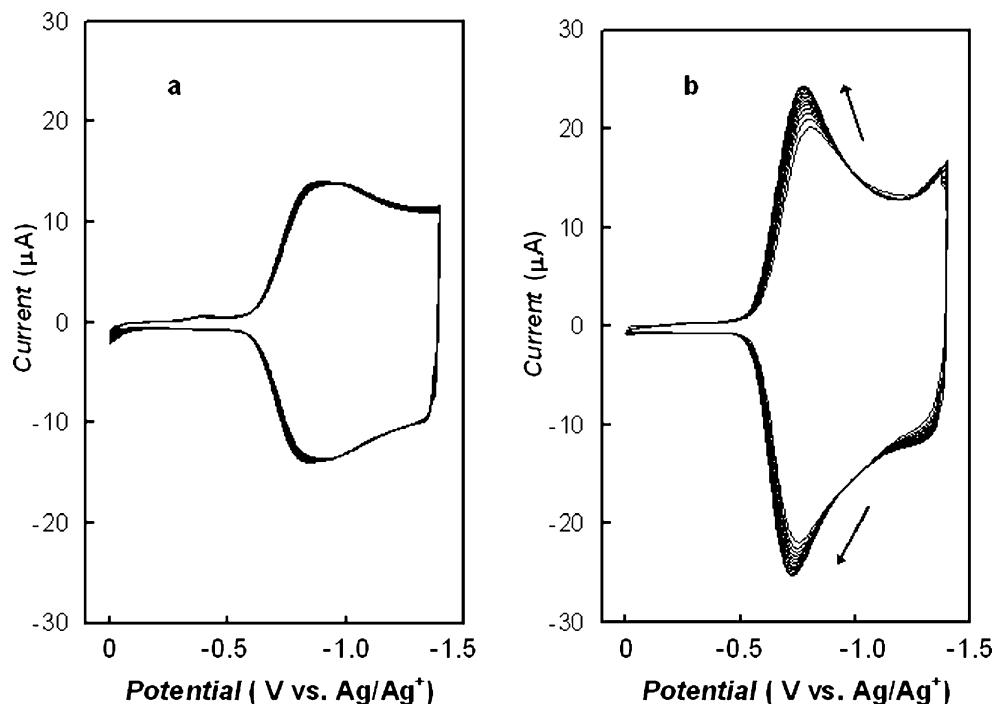


**Fig. 25** Cyclic voltammograms for a *poly-C<sub>60</sub>Pd* film in 0.1 M (*n*-Bu<sub>4</sub>N)ClO<sub>4</sub> in acetonitrile **a** before and **b** after exposure to carbon monoxide. The potential scan rate was 100 mV/s (Winkler and Balch, unpublished results)



the computed structures of these heterofullerenes with the metal atoms substituted for one or two carbon atoms within the fullerene cage. These results demonstrate the prospective application of the *poly-C<sub>60</sub>M* and *poly-C<sub>70</sub>M* polymers for preparation of novel heterofullerenes.

The fullerene-based polymer films were also used for the preparation of bilayer systems at electrodes [130]. Junctions between conducting polymers may serve for charge trapping [131, 132]. A bilayer film, composed of an inner polypyrrole layer and outer *poly-C<sub>60</sub>Pd* layer, is accordingly electroactive over an unusually broad potential range (Fig. 27). As this bilayer film is composed of the *p*-doped (polypyrrole) and *n*-doped (*poly-C<sub>60</sub>Pd*) polymer, it can be used as electroactive material for constructing polymeric batteries. The electrochemical responses of the bilayer films

composed of the *poly-C<sub>60</sub>Pd* and *poly-Fc-C<sub>60</sub>Pd* layers depend upon the sequence of polymeric layers deposited and the conductivity of the inner layer. Doping the inner *poly-C<sub>60</sub>Pd* layer with the metallic palladium nano-particles increases the conductivity of this layer and affects the electrode processes within the bilayer. The voltammetric responses of bilayers composed of the *poly-C<sub>60</sub>Pd* and *poly-Fc-C<sub>60</sub>Pd* layer are shown in Fig. 28.

## Conclusions

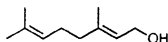
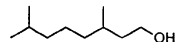
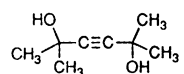
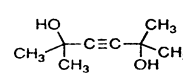
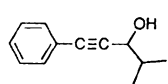
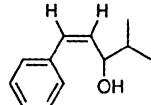
The unique electronic properties of fullerenes, including their good electron-accepting ability, make them an important class of compounds available for the synthesis of different macromolecular systems. Among them, fullerene-based polymers are particularly important. Much of the work in the area of the fullerene-containing polymers is relevant to their potential applications in optical and electrical technology.

So far, chemical synthesis is the most commonly used method for the preparation of fullerene-containing polymers. But electrochemistry has also been extensively used for the synthesis of these materials because it overcomes some possible disadvantages of chemical synthesis. That is, under electrochemical conditions, the rate of polymerization, the structure and the oxidation state of the polymer formed as well as extent of its swelling with a solvent can be easily controlled. The methods of electrochemical

**Table 3** Catalytic hydrogenation of diphenylacetylene (adapted from [125])

Catalyst	Presence of metallic Pd nanoparticles	Reaction half-life time (min)
C <sub>60</sub> Pd <sub>1.44</sub>	No	No reaction
C <sub>60</sub> Pd <sub>2.46</sub>	No	No reaction
C <sub>60</sub> Pd <sub>2.58</sub>	No	No reaction
C <sub>60</sub> Pd <sub>2.71</sub>	No	No reaction
C <sub>60</sub> Pd <sub>2.78</sub>	Yes	330
C <sub>60</sub> Pd <sub>3.37</sub>	Yes	45
C <sub>60</sub> Pd <sub>4.23</sub>	Yes	20
C <sub>60</sub> Pd <sub>6.99</sub>	Yes	13

**Table 4** Hydrogenation of olefins and acetylenes over  $C_{60}Pd_n$  (adapted from [125])

Substrate	Catalyst	Time	Product	Yield (%)
Diphenylacetylene	$C_{60}Pd_{5.05}$	70 min	1,2-Diphenylethane	91
Cyclooctene	$C_{60}Pd_{5.05}$	3 h	Cyclooctane	98
	$C_{60}Pd_{5.05}$	24 h		83
PhCH=CHCH <sub>2</sub> OAc	$C_{60}Pd_{5.05}$	45 min	PhCH <sub>2</sub> CH <sub>2</sub> CH <sub>2</sub> OAc	87
PhCH=CHCO <sub>2</sub> Me	$C_{60}Pd_{5.05}$	2 h	PhCH <sub>2</sub> CH <sub>2</sub> CO <sub>2</sub> Me	95
	$C_{60}Pd_{4.61}$	6 h		80
	$C_{60}Pd_{4.61}$	6 h		76

preparation and properties of fullerene-based polymers have been critically reviewed in the present article.

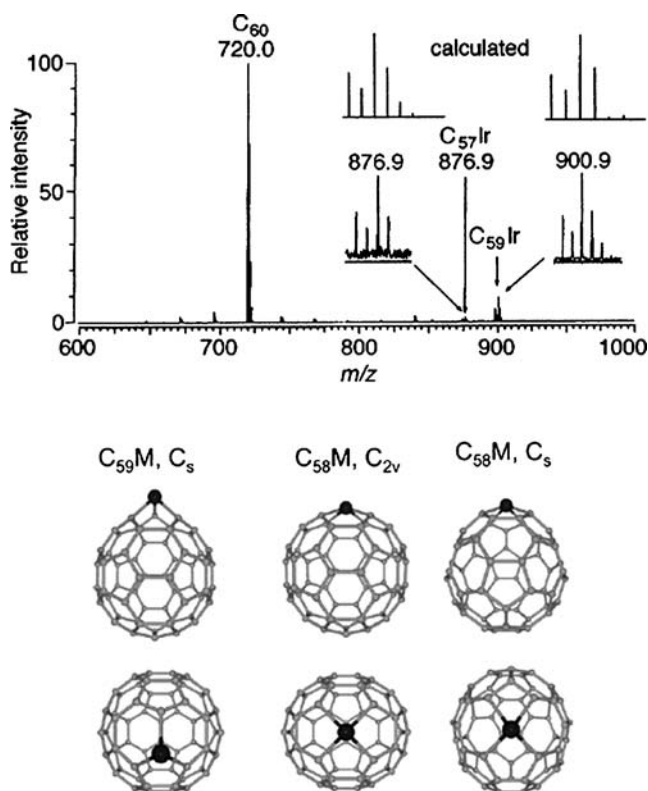


**Fig. 26** Mass spectra (positive ion mode) obtained by laser ablation of  $poly-C_{60}Ir$  film electrodeposited on gold foil from  $C_{60}$  and  $Ir(CO)_2Cl(p$ -toluidyne) and two orthogonal views of the calculated structures of  $C_{59}M$ , the  $C_{2v}$  isomer of  $C_{58}M$  (6:6 C–C bond substitution), and the  $C_s$  isomer of  $C_{58}M$  (6:5 substitution) (adapted from [128] with permission from Royal Chemical Society and [129] with permission from American Chemical Society)

The simplest method of preparation of fullerene polymeric systems consists in entrapment of fullerenes or their derivatives in the polymeric network. However, the structure of these systems is poorly defined. The low stability of these films with respect to repeated potential cycling is another disadvantage of these materials.

The  $C_{60}$  or  $C_{70}$  homopolymers can be prepared by electroreduction of fullerenes in the presence of small alkali metal cations or during fullerene electro-oxidation. In this case, the polymers are formed via ionically induced [2+2] cycloaddition.

Electroreduction of fullerene epoxides also results in the formation of polymeric films on the electrode surface. In the

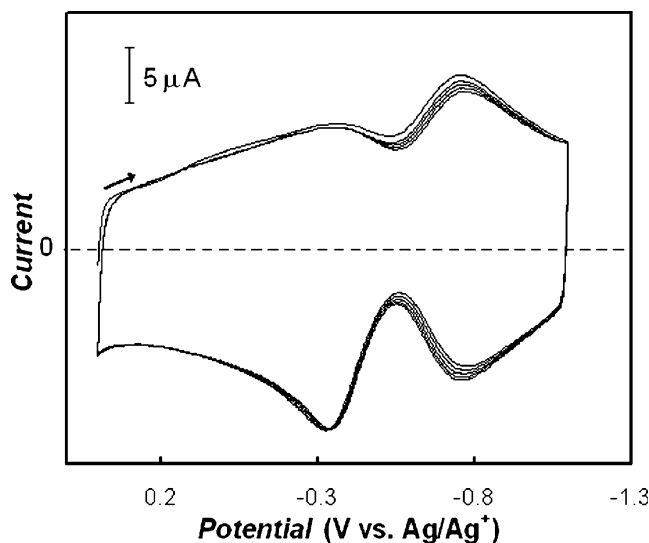


**Fig. 27** Multi-scan cyclic voltammogram of an electrode/polyppyrrrole/ $poly-C_{60}Pd$  bilayer film in 0.1 M ( $n$ -Bu<sub>4</sub>N)ClO<sub>4</sub>, in acetonitrile. The potential scan rate was 100 mV/s (from [130] with permission from Royal Chemical Society)

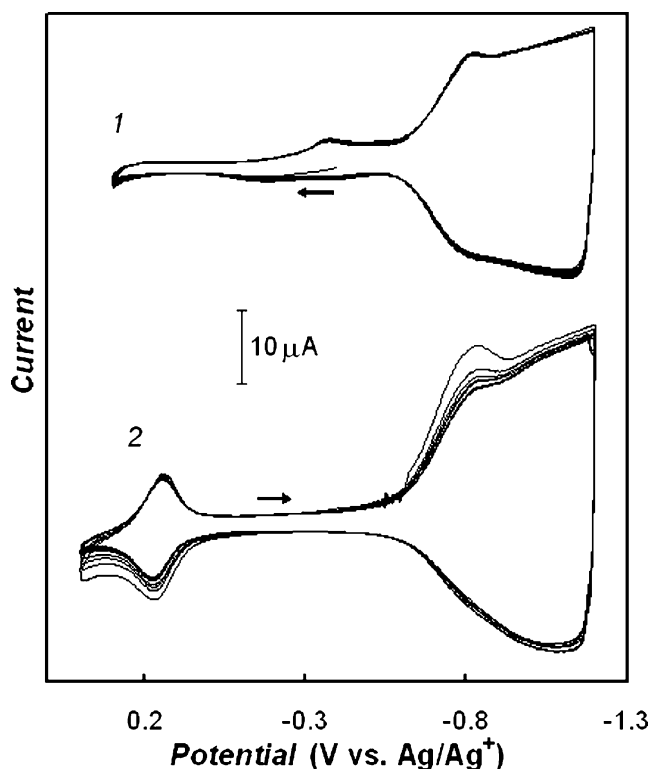


**Fig. 28** Multi-scan cyclic voltammograms for a bilayer film of **1** electrode/*poly*-Fc- $C_{60}$ Pd/*poly*- $C_{60}$ Pd, **2** electrode/*poly*- $C_{60}$ Pd/*poly*-Fc- $C_{60}$ Pd, and electrode/*poly*- $C_{60}$ Pd (doped with Pd nanoparticles)/*poly*-Fc- $C_{60}$ Pd in 0.1 M (*n*-Bu<sub>4</sub>N)ClO<sub>4</sub> in acetonitrile. The potential scan rate was 100 mV/s (Winkler et al., unpublished, results)

polymeric chain,  $C_{60}$  moieties are presumably bound through tetrahydrofuran-like four-membered rings. Moreover, similar films can be prepared by electroreduction of fullerenes in the presence of dioxygen. The structure and electrochemical properties of both types of films are similar. These films can be stable in a relatively wide potential window and their charge-storage capacity is appreciably high.

An important class of polymeric materials is electro-synthesized from monomers containing fullerenes as pendant substituents. In the films formed that way on the electrode surface, the fullerene moieties are covalently bound, for instance, to a polythiophene backbone. These systems feature two mechanisms of charge transport. Electrons can be either transferred through chains in the conjugated polymer or via doping between neighboring fullerene moieties. Therefore, these systems are called “double cables”.

Particular attention has been focused on the formation and properties of polymers comprised of both  $C_{60}$  and transition metal complexes. These polymers can be prepared by electroreduction in solutions containing a variety of metal complexes and fullerenes or chemically modified fullerenes bearing covalent attachments. The surface topol-

ogy, electrochemical properties, and stability of these systems have been thoroughly studied. The *poly*- $C_{60}$ M systems show electrochemically reversible behavior at negative potentials due to electroreduction of the fullerene moieties. Similar materials can be electro-synthesized from fullerene derivatives. Fullerenes covalently derivatized with the electron-donating moieties, such as ferrocene or metal porphyrins, are electroactive both in the negative and positive potential ranges. These polymers also belong to the “double cable” materials. The structure and properties of the *poly*- $C_{60}$ Pd and *poly*- $C_{60}$ Pt films can be altered by the incorporation of palladium or platinum metallic nanoparticles. The metallic phase can participate in heterogeneous charge transfer.

The prospective applications of electrochemically prepared films of polymers built of fullerenes or their derivatives are numerous. These polymers can be used as charge-storage materials in electronic technology. The presence of fullerenes within the polymeric network significantly increases photoconductivity of the polymer. Such systems can be used in solar cells or photodetectors. Fullerene moieties immobilized at the electrode surface in polymer films can mediate electron transfer. Therefore, electrodes coated with the fullerene-based polymers can be used as electrochemical sensors. Films of *poly*- $C_{60}$ Pd and *poly*- $C_{60}$ Pt containing metallic nano-particles of palladium and platinum, respectively, catalyze the hydrogenation of alkenes and alkynes. Moreover, these polymers can be used as absorbents for gases that contain a phenyl ring in their structures. Laser ablation of electrochemically formed *poly*- $C_{60}$ M and *poly*- $C_{70}$ M polymer films (M=Pt or Ir) results in fragmentation of the fullerenes, leading to formation of hetero-fullerenes, such as  $[C_{59}M]^+$  and  $[C_{69}M]^+$ .

**Acknowledgements** Financial support of the Ministry of Education and Science of Poland (Project No. 3T09A04626 to KW and Project No. 4T09A16023 to WK) and the US National Science Foundation (Grant No. CHE 0413857 to ALB) is gratefully acknowledged.

## References

1. Wudl F (2002) *J Mater Chem* 12:1959
2. Rao CNR, Seshadri R, Govindaraj A, Sen R (1995) *Mater Sci Eng* R15:209
3. Wilson LJ, Cagle DW, Thrash TP, Kennel SJ, Mirzadeh S, Alford JM, Ehrhardt GJ (1999) *Coord Chem Rev* 190–192:199
4. Chen Y, Huang ZE, Cai RF, Yu BC (1998) *Eur Polym J* 34:137
5. Prato M (1999) In: Hirsch A (ed) *Fullerene materials in fullerenes and related structures*. Springer, Berlin Heidelberg New York
6. Echegoyen L, Herranz MA, Echegoyen L (2006) *Fullerenes*. In: Bard AJ, Stratmann M (eds) *Encyclopedia of electrochemistry*, vol 7a: inorganic electrochemistry. Scholz F, Pickett CJ (eds), pp 145
7. Bethune DS, Johnson RD, Salem JR, de Vries, MS, Yannoni CS (1993) *Nature* 366:123

8. Takata M, Umeda B, Nishibori E, Sakata M, Saito Y, Ohno M, Shinohara H (1995) *Nature* 377:46
9. Shinohara H (2000) *Rep Prog Phys* 63:843
10. Balch AL, Olmstead MM (1999) *Coord Chem Rev* 185–186:601
11. Guldi DM, Martin N (2002) *J Mater Chem* 12:1978
12. Andersson T, Nilsson K, Sundahl M, Westman G, Wennerstrom O (1992) *J Chem Soc Chem Commun* 604
13. Yoshida ZI, Tatekuma H, Takekuma SI, Matsubara (1994) *Angew Chem Int Ed Engl* 33:1597
14. Boulas P, Kutner W, Jones MT, Kadish KM (1994) *J Phys Chem* 98:1282
15. Atwood JL, Koutsantonis GA, Raston CL (1994) *Nature* 368:229
16. Williams RM, Zwier JM, Verhoeven JW, Nachtegaal GH, Kentgens APM (1994) *J Am Chem Soc* 116:6965
17. Feng W, Miller B (2000) *J Electrochem Soc* 147:2625
18. Atwood JL, Barbour LJ, Raston CL, Sudria IBN (1998) *Angew Chem Int Ed* 37:981
19. Diederich F, Effing J, Jonas U, Jullien L, Plesniviy T, Ringsdorf R, Thilgen C, Weistein D (1992) *Angew Chem Int Ed Engl* 31:1599
20. Olmstead MM, Costa DA, Maitra K, Noll BC, Phollips SL, van Calcar PM, Balch AL (1999) *J Am Chem Soc* 121:709
21. Kubo Y, Sugasaki A, Ikeda M, Sugiyasu K, Sonoda K, Ikeda A, Takeuchi M, Shinkai S (2002) *Org Lett* 4:925
22. Evans DR, Fackler NLP, Xie Z, Rickard CEF, Boyd PDW, Reed CA (1999) *J Am Chem Soc* 121:8466
23. Hawker CJ, Wooley KL, Frechet JMJ (1994) *J Chem Soc Chem Commun* 925
24. Wooley KL, Hawker CJ, Frechet JMJ (1993) *J Am Chem Soc* 115:9836
25. Nierengarten JF, Schall C, Nicoud JF (1998) *Angew Chem Int Ed Engl* 37:1934
26. Chen Y, Huang WS, Huang ZE, Cai RF, Chen SM, Yan XM (1997) *Eur Polym J* 33:823
27. Samulski ET, DeSimone JM, Hunt MO Jr, Menciloglu YZ, Jarnagin RC, York GA, Labat KB, Wang H (1992) *Chem Mater* 4:1153
28. Wignall GD, Affholter KA, Bunick GJ, Hunt MO Jr, Menciloglu YZ, DeSimone JM, Samulski ET (1995) *Macromolecules* 28:6000
29. Bunker CE, Lawson GE, Sun YP (1995) *Macromolecules* 28:3744
30. Yerezian C, Hansen K, Diederich FN, Whetten RL (1992) *Nature* 359:44
31. Ito A, Morikawa T, Takahashi T (1993) *Chem Phys Lett* 211:333
32. Zhou P, Dong ZH, Rao A, Eklund PC (1993) *Chem Phys Lett* 211:337
33. Zhao YB, Poirier DM, Pachman RJ, Weaver JH (1994) *Appl Phys Lett* 64:577
34. Takahashi N, Dock H, Matsuzawa N, Ata M (1993) *J Appl Phys* 74:5790
35. Yamawaki H, Yoshida M, Kakadate Y, Usuba S, Yokoi H, Fujiwara S, Aoki K, Ruoff R, Malhorta R, Lorents DC (1993) *J Phys Chem* 97:11161
36. Rao AM, Zhou P, Wang KA, Hager GT, Holden JM, Wang Y, Lee WT, Bi XX, Eklund PC, Cornett DC, Duncan MA, Amster IJ (1993) *Science* 250:955
37. Stephens PW, Bortel G, Falgel M, Tegze A, Janossy A, Pekker S, Oszanyi G, Forro L (1994) *Nature* 370:636
38. Pekker S, Janossy A, Milhaly L, Chauvet O, Carrard M, Forro L (1994) *Science* 265:1077
39. Koller D, Martin MC, Stephens PW, Milhaly L, Pekker S, Janossy A, Chauvet O, Forro L (1995) *Appl Phys Lett* 66:1015
40. Pekker S, Forro L, Milhaly L, Janossy A (1993) *Solid State Commun* 84:935
41. Grasso G, de Swiet TM, Titman JJ (2002) *J Phys Chem B* 106:8676
42. Loy DA, Assink RA (1992) *J Am Chem Soc* 114:3977
43. Bunker CE, Lawson GE, Sun YP (1995) *Macromolecules* 28:7959
44. Cao T, Webber SE (1996) *Macromolecules* 29:3826
45. Ford WT, Graham TD, Mourey HT (1997) *Macromolecules* 30:6422
46. Hirsch A, Li Q, Wudl F (1991) *Angew Chem Int Ed* 30:1309
47. Geckeler KE, Hirsch A (1993) *J Am Chem Soc* 115:3850
48. Weis C, Friedrich C, Mulhaupt R, Frey H (1995) *Macromolecules* 28:403
49. Sun YP, Liu B, Lawson GE (1997) *Photochem Photobiol* 66:301
50. Hawker CJ (1994) *Macromolecules* 27:4836
51. Rubin Y, Khan S, Freedberg D, Yerezian C (1993) *J Am Chem Soc* 118:344
52. Herrmann A, Diederich F, Thilgen C, ter Meer H, Muller G (1994) *Helv Chim Acta* 77:1689
53. Nie B, Rotello VM (1997) *Macromolecules* 30:3949
54. Xie X, Perez-Cordero E, Echegoyen E (1992) *J Am Chem Soc* 114:3978
55. Xie X, Arias F, Echegoyen E (1993) *J Am Chem Soc* 115:9818
56. Bruno C, Dubitski I, Marcaccio M, Paolucci F, Paolucci D, Zaopo A (2003) *J Am Chem Soc* 125:15738
57. Yoshino K, Morita S, Kawai T, Araki H, Yin XH, Zakhidov AA (1993) *Synth Met* 55–57:2991
58. Down SE, Rosseinsky DR, Whitehouse RS (1994) *J Electroanal Chem* 365:311
59. Carano M, Cosnier S, Kordatos K, Marcaccio M, Margotti M, Paolucci F, Prato M, Roffia S (2002) *J Mater Chem* 12:1996
60. Baril D, Chabre Y (2001) *Electrochem Solid-state Lett* 4:E21
61. Itaya A, Suzuki S, Tsuboi Y, Miyasaka H (1997) *J Phys Chem B* 101:5118
62. Wang Y, Suna A (1997) *J Phys Chem B* 101:5627
63. Gebeheyyu D, Padinger F, Fromherz T, Hummelen JC, Sarcifitei NS (1999) *Int J Photoen* 1:95
64. Yoshino K, Yin XH, Moriata S, Kawai T, Zakhidov AA (1999) *Solid State Commun* 85:85
65. Shaheen SE, Babeer CJ, Padinger F, Fromherz T, Hammelen JC, Sarcifitei (2001) *Appl Phys Lett* 78:841
66. Sun D, Reed CA (2000) *Chem Commun* 2391
67. Strasser P, Ata M (1998) *J Phys Chem B* 102:4131
68. Macaccio M, Bruno C, Fioravanti G, Paolucci F, Paolucci D, Zanarini S, Reed C (2005) 2007th meeting of The Electrochemical Society, Quebec City, Canada, abs. no 825
69. Benincori T, Brenna E, Sonnicolo F, Trimarco L, Zoti G, Sozzani P (1995) *Angew Chem Int Ed Engl* 33:194
70. Cravino A, Zerza G, Neugebauer H, Maggini M, Bucella S, Menna E, Svensson M, Andersson MR, Brabec CJ, Sarcifitei NS (2002) *J Phys Chem B* 106:70
71. Carvino A, Sarcifitei NS (2002) *J Mater Chem* 12:1931
72. Cravino A, Zerza G, Maggini M, Bucella S, Svensson M, Andersson MR, Neugebauer H, Sarcifitei NS (2000) *Chem Commun* 2487
73. Cravino A, Zerza G, Neugebauer H, Bucella S, Maggini M, Menna E, Scorrano G, Svensson M, Andersson MR, Sarcifitei NS (2001) *Synth Met* 121:1555
74. Anderson HL, Boudou C, Diederich F, Gisselbrecht JP, Gross M, Seiler P (1994) *Angew Chem Int Ed Engl* 33:1628
75. Nierengarten JF (2002) In: Guldi DM, Martin N (eds) *Fullerenes: from synthesis to optoelectronic properties*. Kluwer, Dordrecht, pp 51–79
76. Prato M, Maggini M (1998) *Acc Chem Res* 31:519
77. Zhang F, Svensson M, Andersson MR, Maggini M, Bucella S, Menna E, Inganas O (2001) *Adv Mater* 13:1871
78. Stevens MP (1999) In: *Polymer chemistry*. Oxford University Press, Oxford, pp 326–329

79. Balch AL, Costa DA, Lee JW, Noll BC, Olmstead MM (1994) *Inorg Chem* 33:2071
80. Elemes Y, Silverman SK, Shen C, Kao M, Foote CS, Alvarez MM, Whetten RL (1992) *Angew Chem Int Ed Engl* 31:351
81. Balch AL, Costa DA, Noll BC, Olmstead MM (1995) *J Am Chem Soc* 117:8926
82. Fedurco M, Costa DA, Balch AL, Fawcett WR (1995) *Angew Chem Int Ed Engl* 34:194
83. Winkler K, Costa DA, Balch AL, Fawcett WR (1995) *J Phys Chem* 99:17431
84. Winkler K, Costa DA, Fawcett WR, Balch AL (1997) *Adv Mater* 9:153
85. Krinichnaya EP, Moravsky AP, Efimov O, Sobczak JW, Winkler K, Kutner W, Balch AL (2005) *J Mater Chem* 15:1468
86. Taylor R, Barrow MP, Drewello T (1998) *J Chem Soc Chem Commun* 2497
87. de Bettencourt-Dias A, Winkler K, Fawcett WR, Balch AL (2003) *J Electroanal Chem* 549:109
88. Balch AL, Olmstead MM (1998) *Chem Rev* 98:2123
89. Nagashima H, Nakaoka A, Saito Y, Kato M, Kawanishi T, Itoh K (1992) *J Chem Soc Chem Commun* 377
90. Nagashima K, Yamaguchi H, Kato Y, Saito Y, Haga MA, Itoh K (1993) *Chem Lett* 2153
91. Nagashima K, Kato Y, Yamaguchi H, Kiura E, Kawanishi T, Kato M, Saito Y, Haga M, Itoh K (1994) *Chem Lett* 1207
92. Wijnkoop MY, Maidine MF, Avent AG, Darwish AD, Kroto HW, Taylor R, Walton DRM (1997) *J Chem Soc Dalton Trans* 675
93. Balch AL, Costa DA, Winkler K (1998) *J Am Chem Soc* 120:9614
94. Hayashi A, de Bettencourt-Dias A, Winkler K, Balch AL (2002) *J Mater Chem* 12:2116
95. Winkler K, Noworyta K, Kutner W, Balch AL (2000) *J Electrochem Soc* 147:2597
96. Winkler K, de Bettencourt-Dias A, Balch AL, Kutner W, Noworyta K (2000) In: Fukuzumi S, D'Souza F, Guldi DM (eds) *Fullerenes, vol 8—electrochemistry and photochemistry*. The Electrochemical Society, Pennington, pp 31–42
97. Winkler K, de Bettencourt-Dias A, Balch AL (1999) *Chem Mater* 11:2265
98. Winkler K, de Bettencourt-Dias A, Balch AL (2000) *Chem Mater* 12:1386
99. Winkler K, Noworyta K, Sobczak JW, Wu CT, Chen CL, Kutner W, Balch AL (2003) *J Mater Chem* 23:518
100. Plonska ME, de Bettencourt-Dias A, Balch AL, Winkler K (2003) *Mater Chem* 15:4122
101. Plonska ME, Makar A, Winkler K, Balch AL (2004) *Pol J Chem* 78:1431
102. Plonska M, Winkler K, Gadde S, D'Souza F, Balch AL (2004) In: Kamat PV, Guldi DM, D'Souza F, Fukuzumi S (eds) *Fullerenes and nanotubes, vol 14—materials for the new chemical frontier*. The Electrochemical Society, Pennington
103. Winkler K, Plonska-Brzezinska ME, Gadde S, D'Souza F, Balch AL (2006) *Electroanalysis* 18:841
104. Diaz AF, Castillo JI, Logan JA, Lee WY (1981) *J Electroanal Chem* 129:115
105. Zhang W, Domg S (1993) *Electrochim Acta* 38:441
106. Rubinstein I, Sabatini E, Rishpon J (1987) *J Electrochem Soc* 134:3078
107. Genies EM, Tslantavis C (1985) *J Electroanal Chem* 195:109
108. Kaneto K, Yoshino K, Inuishi J (1983) *Jpn J Appl Phys* 22:567
109. Ferraris JP, Eissa MM, Brotherston ID, Loveday DC, Moxry AA (1998) *J Electroanal Chem* 459:57
110. Mastragostino M, Soddu L (1990) *Electrochim Acta* 35:463
111. Dalton EF, SurrIDGE NA, Jemigan JC, Wilbourn KO, Facci JS, Murray RW (1990) *Chem Phys* 141:143
112. Kawabe S, Kawai T, Sugimoto R, Yagasaki E, Yoshino K (1997) *Jpn J App Phys* 36:L1055
113. Burke A (2000) *J Power Sources* 91:37
114. Alekseev AS, Tkachenko NV, Tauber AY, Hynninen PH, Osterbacka R, Stubb H, Lemmetyinen H (2002) *Chem Phys* 257:243
115. Vuorinen T, Kaunisto K, Tkachenko NV, Efimov A, Lemmetyinen H (2006) *J Photochem Photobiol A Chem* 178:185
116. Sariciftci NS, Braun D, Zhang C, Srdanov VI, Heeger AJ, Stucky G, Wudl F (1993) *Appl Phys Lett* 62:585
117. Tu G, Wang J, McElvain J, Heeger AJ (1998) *Adv Mater* 10:1431
118. Sherigara BS, Kutner W, D'Souza F (2003) *Electroanalysis* 15:753
119. Patolsky F, Tao G, Katz E, Willner I (1998) *J Electroanal Chem* 454:9
120. Gavalas VG, Chanioyakis NA (2000) *Anal Chim Acta* 409:131
121. Li M, Xu M, Gu Z, Zhou X (2002) *J Phys Chem B* 106:4197
122. Tien HT, Ottova AL (1998) *Electrochim Acta* 43:3587
123. D'Souza F, Rogers LM, O'Dell ES, Kochman A, Kutner W (2005) *Bioelectrochemistry* 66:35
124. Nagashima H, Nakaoka A, Tajima S, Saito Y, Itoh K (1992) *Chem Lett* 1361
125. Yu R, Liu Q, Tan KL, Xu GQ, Ng SC, Chan HSO, Hor TSA (1997) *J Chem Soc Faraday Trans* 93:2207
126. Hayashi A, Tamamoto S, Suzuki K, Matsuoka T (2004) *J Mater Chem* 14:2633
127. Poblet JM, Munoz J, Winkler K, Cancilla M, Hayashi A, Lebrilla CB, Balch AL (1999) *Chem Commun* 493
128. Hayashi A, Xie Y, Poblet JM, Campanera JM, Lebrilla CB, Balch AL (2004) *J Phys Chem A* 108:2192
129. Campanera JM, Bo C, Balch AL, Ferré J, Poblet JM (2005) *Chem Eur J* 11
130. Wysocka M, Winkler K, Balch AL (2004) *J Mater Chem* 14:1036
131. Torres W, Fox MA (1990) *Chem Mater* 2:306
132. Berchmans S, Usha S, Ramalechume C, Yegnaraman V (2005) *J Solid State Electrochem* 9:595